Response to “RC2: 'Comment on egusphere-2025-4771', Christian Wild, 21 Jan 2026”

Dear Dr. Wild,

We thank you for reviewing our manuscript and for providing a thoughtful, detailed, and insightful critique of our approach to exploring glaciological processes. In response to your major comments, we conducted: 1) additional ice-bending analysis, 2) improved ice surface displacement reconstruction, and 3) revision to our analysis and discussion of flexure-zone and grounding-zone widths and their landward positions. We hope that these changes, along with minor revisions, have improved both the quality and scope of the manuscript, and, in particular, its relevance to the cryospheric modeling community.

Our detailed responses to all comments are provided below in blue font.

Review of Antropova et al., submitted to The Cryosphere Discussion
Intra-annual grounding line migration and retreat: insights from high-resolution satellite and in-situ observations over Milne Glacier in the Canadian High Arctic
By Christian T. Wild
January 2026

Summary:
Antropova et al. present a detailed differential interferometric SAR (DInSAR) analysis of the tidal-flexure zone of Milne Glacier. Using a high-temporal-resolution RADARSAT dataset with 4-day repeat intervals, combined with in situ observations, they test the commonly assumed steady-flow condition applied in many DInSAR grounding-line studies. They also show that intra-annual grounding-line retreat occurs in a spatially and temporally heterogeneous pattern. They link this variability to subglacial topography and the development of localized pinning points, and offer speculations about the implications for basal melt rates and the potential for upstream ocean-water intrusion beneath the ice.

Strengths:
The authors demonstrate strong command of the DInSAR technique from a remote-sensing perspective and reveal clear, instructive examples of well-known processes associated with tidal flexure of ice shelves, which I elaborate on below. I have rarely seen such a thorough quantification of the steady-flow assumption, nor such careful consideration of how different satellite tracks (and associated variations in incidence angle and azimuth) capture the tidal-flexure signal. For this, I commend the authors. I particularly appreciate their use of available GNSS data for validation. However, because the GNSS measurements may be temporally biased (limited to a three-hour acquisition window per day, L183, which may also explain why they yield substantially higher ice velocities than the SAR-derived estimates in Fig. 2a), I wonder whether the analysis should be extended to include SAR-derived velocities alone. This would make the approach more transferable to settings where GNSS data are unavailable and could provide a clearer spatial picture of how the steady-flow assumption performs across the tidal-flexure zone, where velocity gradients are most pronounced towards their lateral margins.

Thank you for your feedback on our study and for recognizing its strengths in the remote sensing component and the use of in situ observations. We consider the use of in situ observations, including GNSS-derived velocities, to be an essential component of this work. We assume the GNSS-derived velocity records to be representative of grounding-zone velocities along the glacier centreline. We have clarified our use of GNSS records in our response below as well as in the manuscript. In addition, we improved our discussion of temporal biases with respect to SAR data acquisition times and quantified uncertainties associated with the derived velocities and tidal bending.
Although SAR-derived velocities provide promising research avenues, we consider this analysis to be outside the scope of the current manuscript. Therefore, SAR-derived velocities are used mainly to support our GNSS-derived velocities, which have much better temporal resolution and are well suited to our DInSAR analysis.

Weaknesses:
The study lacks a clearly defined glaciological hypothesis and instead reads largely as an enumeration of observations that have been explored extensively in the past.. Similar datasets have already been used to address, among other things: (1) improvements to tidal models (Wild et al., 2019), (2) the depth of the neutral layer in a deforming beam, (3) effective ice stiffness (Wild et al., 2018), (4) shear-margin strength (Wild et al., 2025), (5) two-dimensional effects on flexural patterns (Rack et al., 2017; Wild et al., 2018). Many of these applications have been published in this journal, yet the authors appear to be insufficiently engaged with this literature. This is reflected in an incomplete reference list, shortcomings in the introduction, and at times imprecise or incorrect terminology.
Given these issues, and considering that most recent glaciological DInSAR studies in *The Cryosphere* now combine DInSAR with multi-sensor approaches (Li et al., 2023), machine-learning methods (Ramanath et al., 2025), broad spatial (Picton et al., 2023) or temporal coverage (Chien et al., 2026), or numerical modeling of tidal flexure (Ross et al., 2024; Wild et al., 2025), I recommend that this manuscript may be more suitably placed in a more method-focused journal such as IEEE or a similar outlet. In that context, it would serve as an excellent technical reference that showcases the paper's considerable methodological strengths. If the manuscript were to be framed more explicitly within a glaciological scope, it could be strengthened by a robust investigation of short-term ice-flow dynamics and their relationship to changing buttressing as pinning points emerge and evolve.

Thank you for the constructive critique and suggestions. We agree that our study has an observational remote-sensing focus. It provides a thorough investigation and quantification of SAR-detected changes in a tidal-flexure zone from four different orbits at a high spatial and temporal resolution, which have not previously been explored in the literature. Our comprehensive dataset and approach contribute to a better understanding of the impact of variable glacier velocity with respect to different SAR viewing geometries on the delineation of SAR-derived tidal flexure-zones. In addition, we explore changes in the tidal flexure zone with respect to environmental and glacier-specific factors. Our advances in these regards should be of interest to the broader glaciological community and well-aligned with The Cryosphere's scope. Therefore, we believe that our study is a better fit for The Cryosphere than for IEEE or a similar outlet.
We acknowledge that the initial version of the manuscript did not explicitly discuss the processes examined in detail by Wild et al. (2018, 2019, 2025) and Rack et al. (2017). To address comments

regarding the processes acting in the glacier flexure zone and to situate our study more clearly within a glaciological context, we have:

- incorporated an analysis of ice compression and extension effects due to bending (i.e., Major Comment 1 below),
- included all sinusoids in the unraveling/reconstruction (i.e., Major Comment 2 below), and
- revised our analysis and discussion of flexure-zone width and hinge-line landward migration, referred to as the "distance to hinge line" (i.e., Major Comments 3 and 4 below).

We also recognize the recent trend in DInSAR-based grounding-line studies toward automated machine learning methods, the use of multiple sensors and/or broader spatial coverage, and integration with modeling, particularly in The Cryosphere. However, our high-temporal-resolution observations of the glacier flexure zone, which explain the short-term drivers of grounding-line migration and suggest the mechanisms of its long-term retreat due to ice deterioration around pinning points, are also of interest to the cryospheric community. In particular, our integrates multiple data types, presents high-spatiotemporal-resolution observations of glaciological processes from a SAR platform, offers insights about glaciological application of DInSAR methodology and its steady flow assumption with respect to SAR viewing geometry, and has implications for glaciers well beyond our study site.

In addition, we considered machine learning methods for automated flexure-zone delineation introduced by Mohajerani et al. (2021). However, this approach has limitations and can be problematic in areas with non-standard fringe patterns, such as pinning points, particularly in high-noise areas that are close to decorrelation (e.g., Fig. 9 in Ramanath et al., 2025). Therefore, we opted for a manual delineation approach to accurately document the emergence of a pinning point on the eastern margin of Milne Glacier.

We also note that many recently published grounding-line studies, including those cited above (Li et al., 2023; Ramanath et al., 2025; Picton et al., 2023; Chien et al., 2026; Ross et al., 2024; Wild et al., 2025) focus on Antarctica and/or Greenland. Our work contributes to improved representation of Arctic glaciers outside of Greenland, that are relatively understudied. These glaciers may serve as analogues for the future evolution of marine-terminating glaciers in Greenland and Antarctica, given their rapid retreat and disintegration, as discussed in our Introduction.

Regarding the comment that our terminology was at times "imprecise or incorrect," we attribute this primarily to inconsistencies in terminology across the literature (i.e., discrepancies between the oceanographic grounding zone and DInSAR grounding zone as detailed in our responses to terminology-related comments from both reviewers), rather than to insufficient engagement with studies published in The Cryosphere. We have revised the terminology throughout the manuscript to address these concerns and to clarify our usage.

The additional analyses addressing the major comments, together with the revisions to the manuscript text addressing the minor comments, have substantially strengthened the paper and enhanced its relevance to the broad readership of The Cryosphere.

Major comments:

1) <u>The bending effect introducing spurious signals in the tidal-flexure zone</u>

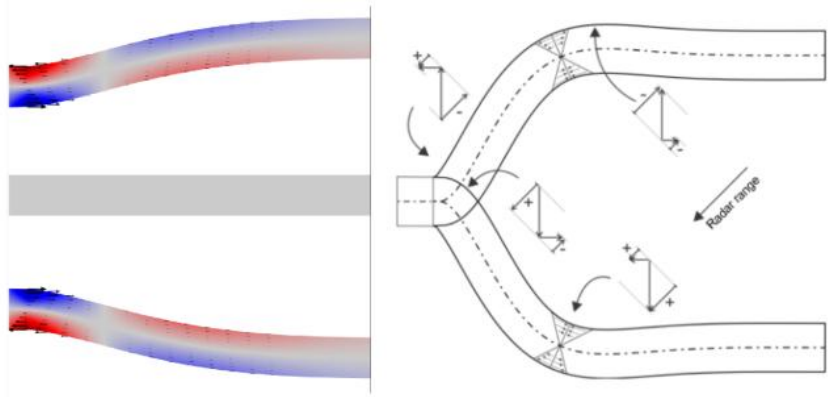

Figure R1: (left) from Wild et al., 2018, (right) from Rack et al., 2017. Red illustrates compression, blue horizontal extension. Arrows indicate magnitude and direction of geometric displacement around a neutral-layer.

The interpretation of individual DInSAR observations warrants more careful consideration of the vertical structure of tidal flexure. These measurements are inherently limited to the ice surface, whereas flexural deformation occurs about a neutral layer located approximately midway through the ice thickness (as illustrated in Fig. R1). In that schematic, the upper part of the beam moves to the left (red) while the lower part moves to the right (blue), highlighting that the ice deforms in opposite directions above and below the neutral layer. Vice versa for low tide as also illustrated. As a result, the surface experiences a harmonic back-and-forth motion during
the tidal cycle, which can generate an apparent, spurious grounding-line migration on the order of one local ice thickness (Rack et al., 2017), which is within the y-range of the scatter presented in Fig. 9a.

This effect is further complicated in two dimensions by grounding-line sinuosity (Wild et al., 2018), which modifies the surface flexure pattern relative to a simple one-dimensional beam (it's dampened within embayments, and propelled around protrusions of the grounding line). In principle, this "bending effect" can be quantified and subtracted using a simple elastic model (with the temporal mean grounding line position, an ice thickness map and the DSSH). The tidal-flexure slopes in both the x and y directions are then combined with assumptions about the distance to the neutral layer. The corresponding x and y components of the bending effect can then be rotated into the radar line-of-sight using straightforward trigonometric relationships.

$$\int_x \delta_x \, dx = Be_x = \frac{H}{2} w'_x$$
$$\int_y \delta_y \, dy = Be_y = \frac{H}{2} w'_y.$$

Given the importance of this effect for grounding-line interpretation, the manuscript would benefit from a more explicit treatment of how surface flexure, the position of the neutral layer, and two-dimensional grounding-line geometry influence the inferred grounding-line signal.

In particular, I am concerned that the delineation of the tidal-flexure zone may be partly biased. Support for this interpretation is provided by the observation that DInSAR-derived displacements acquired at higher incidence angles show improved correlation during the unstable regime (Fig. 8a/b and L319–321). As the radar incidence angle increases, the sensor becomes more sensitive to horizontal surface motion and its temporal variability, which amplifies the contribution of geometric surface deformation associated with flexure, compared to a lower incidence angle.

This also has implications for the authors' conclusion that "a larger grounding-zone width promotes increased ice flow" (L443-445). Thicker ice is expected to exhibit a more pronounced bending effect than thinner ice, and the associated geometric surface motion should be greatest at the grounding line itself, where curvature is most pronounced. This could, at least in part, create or exaggerate the appearance of a wider grounding zone independent of dynamic ice flow.

For this reason, the multi-incidence-angle DInSAR dataset presented in the manuscript offers a valuable opportunity. The differing sensitivity of the observations to horizontal versus vertical motion provides a promising, and untapped, means of constraining the depth of the neutral layer beneath the ice surface. Such an analysis would also represent a significant contribution to ongoing glaciological efforts to infer basal melt rates from phase-sensitive radar measurements in the tidal-flexure zone (Vaňková et al., 2020).

Thank you for suggesting an analysis of the effect of bending on DInSAR-derived surface displacement. We have implemented the elastic model described by Rack et al. (2017), using known thickness values along the three transects. An example of horizontal surface displacement along the central transect, associated with the highest and lowest tides during the observation period, is shown in Fig. 1AR.

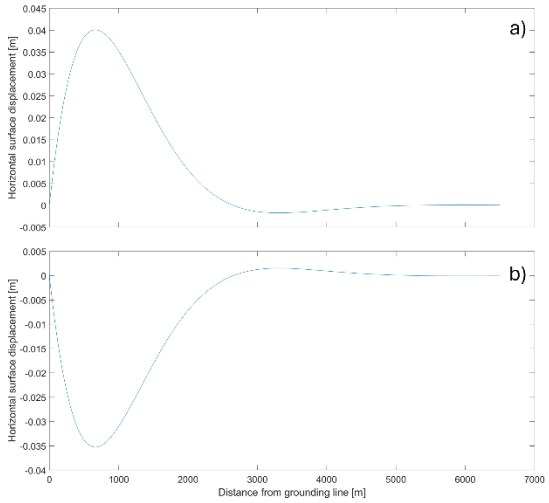

Figure 1AR: Horizontal surface displacements assuming an ice thickness of 210 m (i.e., the mean thickness of the grounding zone along the central transect) and an elastic Young's modulus of 1.5 GPa for (a) the highest tide of 0.50 m and (b) the lowest tide of −0.44 m during the observation period.

Using this simple elastic model, we assessed the contribution from differences in ice stretching or compression caused by tides at the times of SAR data acquisition. We then quantified these

contributions for all orbits ("MeanLOSbend error" in Fig. 2AR). As expected, the most pronounced contribution from horizontal displacement due to velocity variability and bending was associated with orbit 09 (high incidence angle, descending pass). We added information about the associated errors, represented as ± distance to the delineated hinge lines/flexure zones, and revised the corresponding text in the manuscript accordingly.

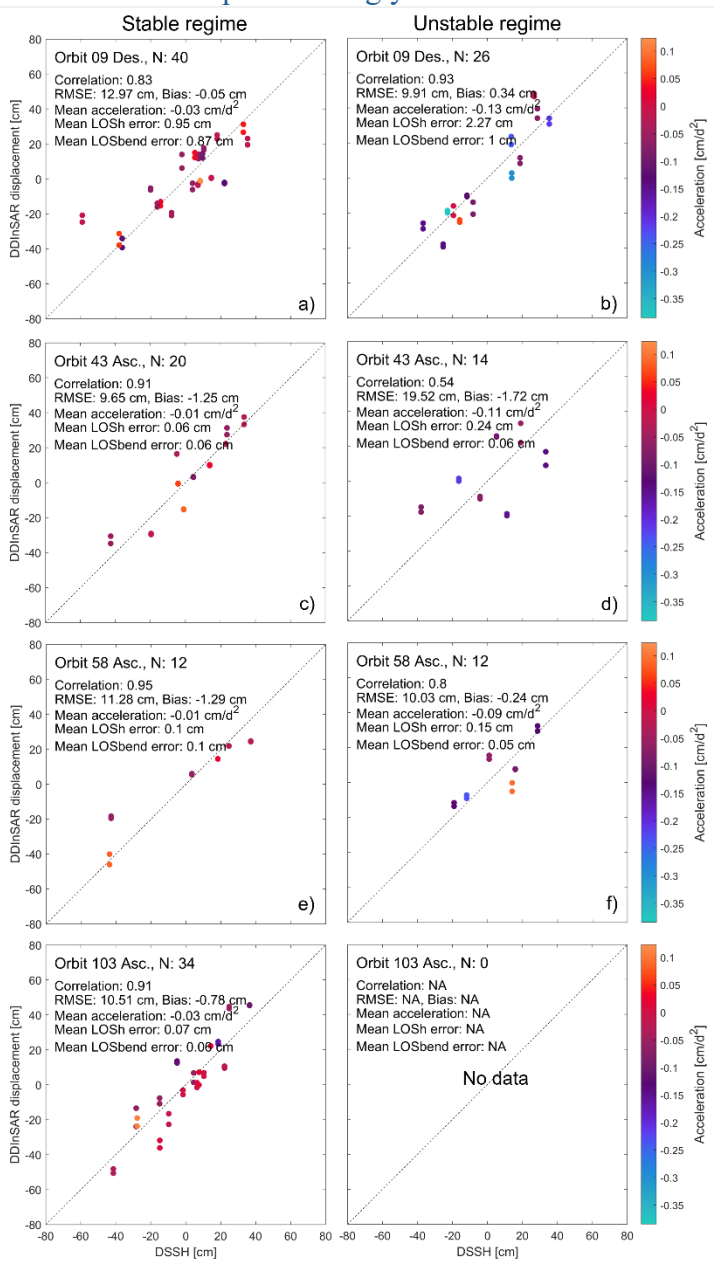

Figure 2AR (updated Fig. 8 from the initial manuscript): DInSAR-derived displacements versus DSSH with respect to glacier velocity regime periods and SAR orbits.

2) Unraveling (here called reconstruction) of DInSAR to single tides

The authors correctly note that DInSAR images represent a double difference of three or four consecutive SAR acquisitions, each taken at different phases of the tidal cycle and therefore containing contributions from multiple tidal constituents as well as atmospheric effects. Consequently, a direct comparison between tide models and DInSAR observations requires either that the same SAR differencing procedure be applied to the modeled tides (as in Fig. 4), or that the DInSAR signal be decomposed into individual tidal components (as attempted in Fig. 6).

The authors pursue the latter approach by fitting a single harmonic with a prescribed angular frequency corresponding to one dominant tidal constituent, both with and without the inclusion of the inverse barometer effect (IBE). While the fit does improve when the IBE is included (Fig. 6), this improvement is expected and has been demonstrated in numerous previous work (e.g., Rignot et al., 2000; Padman et al., 2003; Wild et al., 2022). Importantly, the remaining root-mean-square error (~13 cm; Fig. 6b/c) remains large relative to the total displacement range of approximately -40 to +60 cm in the corresponding double-difference interferograms (Fig. 5a). In my view, this relative magnitude of residual error limits the physical interpretability of the harmonic decomposition using a single sinusoid. I would also like to draw the author's attention to (Minchew et al., 2017), who underscore the importance of using all sinusoids for the unraveling/reconstruction (with former knowledge of their phase from GNSS).

In previous work, we developed and applied an alternative approach for unraveling DInSAR to single tides for Darwin Glacier (Wild et al., 2019) and subsequently for Priestley Glacier (Wild et al., 2025), both published in *The Cryosphere*. This method uses the mean tide-deflection ratio (the so-called alpha map first introduced by Han and Lee, 2015) to separate DInSAR observations into individual tidal components, reducing the residual RMSE to a level comparable to interferometric noise (on the order of 1 cm for Sentinel-1). Based on the flexure curves shown in Fig. 5, the Milne Glacier dataset appears well suited for this type of analysis, and its application here could substantially strengthen the study and its glaciological scope. In this context, relying solely on a single-harmonic fit, despite recognizing the importance of IBE forcing, seems a missed opportunity to fully exploit the dataset. I would be very willing to discuss or advise on such an analysis if helpful, while recognizing that this would extend beyond the minimum expectations for a reviewer.

Two additional benefits of the alpha-map approach are worth noting. First, it naturally averages over the bending effect associated with the position of the neutral layer, because DInSAR observations sample all phases of the tidal cycle (as illustrated in Fig. 5). Second, it mitigates the influence of viscoelastic effects, which appear to be present in several flexure curves along the West and Central transects, through temporal averaging (discussed further below), so it avoids the implementation of a numerical model.

Our manuscript focuses on the "standard" DInSAR method and its assessment with respect to horizontal displacement components caused by variable velocity and bending effects (added in the revised version of the manuscript). Therefore, we consider the alpha-map approach to be outside the scope of this manuscript.
However, based on the feedback above, we improved our initial least-squares fitting approach by including all tidal constituents (i.e., 59) computed using the T_TIDE algorithm (Pawlowicz et al., 2002). The coefficients for each harmonic component were estimated using a regularized least-

squares approach. To minimize the effect of horizontal displacement in our DInSAR results, the reconstruction was performed only for the stable season.
As a result, the remaining RMSE decreased from ~13 cm to ~5 cm (Fig. 3AR, lower panels), which is a substantial improvement. Moreover, given that T_TIDE shows a correlation of 0.96 and an RMSE of 3.4 cm with our in situ tidal observations (details provided in the corresponding comment below), the remaining RMSE of ~5 cm in our reconstruction analysis is reasonable.

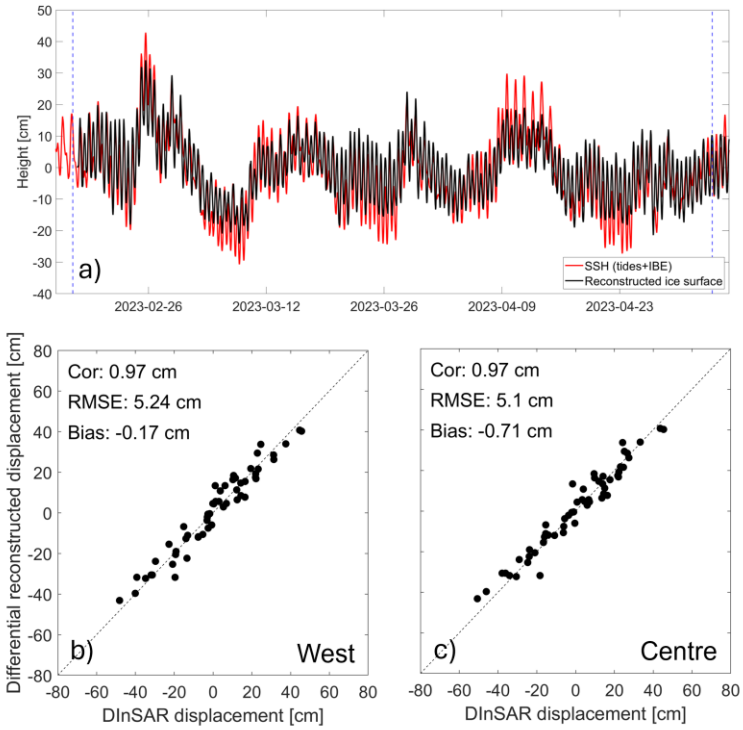

Figure 3AR (updated Fig. 6 from the initial manuscript): Preliminary figure of reconstructed ice surface height.

3) Tidal forcing and flexure-zone width

I would appreciate further clarification regarding the physical basis for the reported relationship between flexure-zone width and the magnitude of the tidal forcing. From my understanding, for a given tidal forcing, the width of the flexure zone should primarily depend on ice stiffness, which is itself governed by ice thickness and the effective Young's modulus (Fig. R2). Under this framework, the magnitude of the tidal forcing should affect displacement amplitudes, but not the spatial extent of the flexural response. Similar for ice viscosity, which affects the timing and shape of the flexure, but not its horizontal extent.

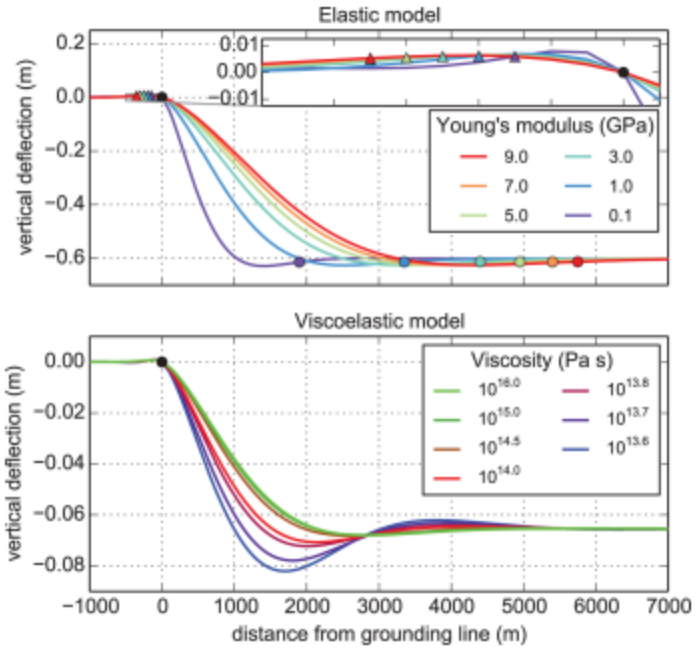

Fig. R2: from Wild et al., 2017. Both panels show that for a given tidal forcing (here -0.6 m) and ice thickness, the flexure-zone width is only dependent on the Young's Modulus. Ice viscosity affects the shape and timing of the flexural wave.

For this reason, I am concerned about the interpretation presented in Fig. 9b, as well as the conclusions drawn from it, may not be physically well founded. In addition, it is unclear whether the linear relationships shown are statistically significant. While some structure is visible in the scatterplot, this pattern may alternatively reflect temporal aliasing in the SAR-data acquisitions, potentially related to tidal phase or inverse barometer effects at the time of SAR-data collection.

To explore this possibility, it would be helpful if the authors could reproduce the classification used in Fig. 2a (i.e., the different triangle symbols) in Fig. 6a and explicitly assess whether systematic biases arise from the timing of the SAR-data acquisitions relative to tidal forcing and IBE. Such an analysis would help to clarify whether the observed relationship reflects a physical signal or an acquisition-related artifact.

We agree that the width of the flexure zone depends on ice stiffness, which is governed by ice thickness and the effective Young's modulus, in turn defined by tensile and compressive stresses. We also think that glacier geometry (i.e., slope steepness and/or direction, i.e., retrograde or prograde, and the presence of pinning points) affects the distribution of tensile and compressive stresses in the flexure zone, as well as its resulting width under varying tides, which is likely nonlinear. Our aim was not to fit a linear function but to demonstrate the presence of an appreciable trend with a moderate correlation (~ 0.4).

We added the requested figure (Fig. 4AR) showing SAR data acquisition times to assess potential temporal aliasing. Additionally, we show the association between DInSAR surface displacement and flexure zone width (Fig. 5AR) for different orbits. We find no obvious evidence of temporal

aliasing due to timing. We removed Figure 9 to avoid potential misinterpretation regarding linear fitting, added a table summarizing the flexure zone span across the transects, and revised our discussion to take the suggested comments into account.

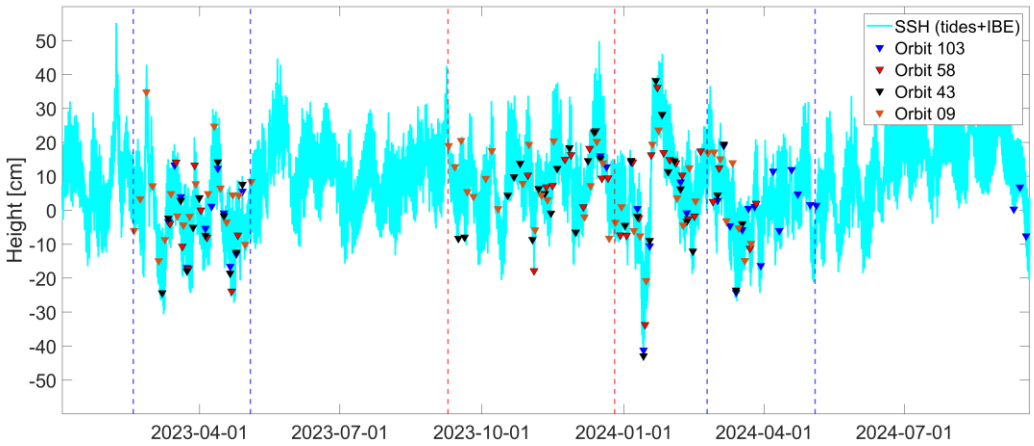

Figure 4AR: SAR data acquisition times with respect to sea surface heights during the 2023-2024 stable season.

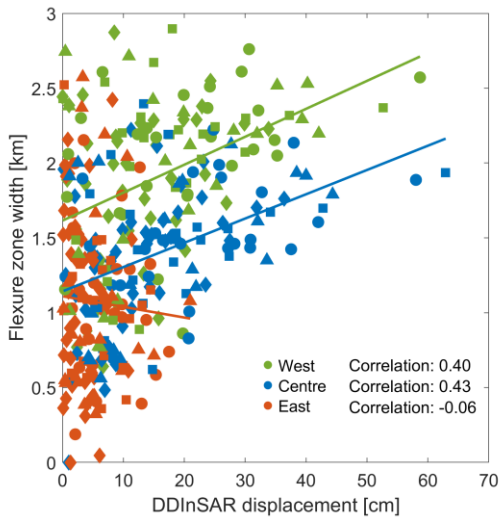

Figure 5AR: Association between DInSAR surface displacement and flexure zone width. Orbit 09 is shown with diamonds, orbit 43 with circles, orbit 58 with squares, and orbit 103 with triangles.

4) Tidal forcing and grounding-zone width

Furthermore, the manuscript presents a similar analysis relating tidal forcing to grounding-zone width (referred to as the "Distance to HL" in Fig. 9a). This type of correlation implicitly assumes that tidal flexure responds instantaneously to the forcing, i.e., that the ice behaves purely elastically. However, at tidal frequencies, glacier ice is well known to exhibit viscoelastic behavior (e.g., Reeh et al., 2003; Wild et al., 2017). Under such conditions, a time lag between the tidal forcing and the flexural response is expected. Importantly, this delay is not constant but is

anticipated to increase nonlinearly from the freely floating portion of the ice shelf toward the grounding (hinge) line.

This viscoelastic response provides a plausible alternative explanation for the observed negative correlations. Time delays on the order of tens of minutes to several hours have been reported in similar settings and should be carefully accounted for when interpreting correlations between tidal forcing and grounding-zone metrics. In this context, applying a simple linear fit across all observations may not be physically appropriate.

A useful first step toward quantifying this time delay would be to correlate the available GNSS observations acquired within the tidal-flexure zone with an independent tide model representative of the freely floating ice shelf. For example, the Gr1kmTM model by Howard and Padman (2021) could be used for this purpose. Introducing an artificial time lag and identifying the lag that maximizes correlation between the modeled tides and the GNSS data, following an approach similar to that described by Wild et al., 2025, would help to assess the magnitude and spatial variability of the viscoelastic response. Such an analysis could substantially strengthen the physical interpretation of the results presented in Fig. 9a.

Similarly to the correlation discussed above (Fig. 5AR), we do not aim to fit a linear function but only to demonstrate the presence of a trend and a moderate correlation. In addition, our analysis of SSH with respect to DInSAR results, divided into two groups (i.e., “notch present” and “no notch”) confirms that the grounding line migrates farther inland (i.e., when a “notch” is present and, thus, the distance to the hinge line is shorter) under high SSH.

We also note that our simulated tides are representative of a freely floating ice shelf based on pressure records from an RBR Duet datalogger moored in a lateral bay. Furthermore, the T_TIDE simulated tides showed better agreement with in situ observations than the Gr1kmTM model (details are provided in our response to the corresponding question below).

To quantify the time delay between the simulated tides and the ice flexure response, we calculated the correlation between the simulated tides and GNSS records using different time shifts (Fig. 6AR). The maximum correlation achieved is about 0.2 with a time shift of 15 minutes (Fig. 6AR c). This low correlation is influenced by the limited GNSS observations and their own oscillations (Fig. 6AR b). Since our GNSS records were collected for only three hours, they unfortunately did not capture a full tidal period, preventing reliable quantification of the correlation and the time shift. Therefore, we prefer to remove Figure 9 to avoid potential misinterpretation, add a table with “Distance to hinge line” values (similar to Table 2), and retain our discussion of how pinning points affect flexure zone width and grounding line inland migration across the glacier, taking into account the suggested perspective of viscoelastic response.

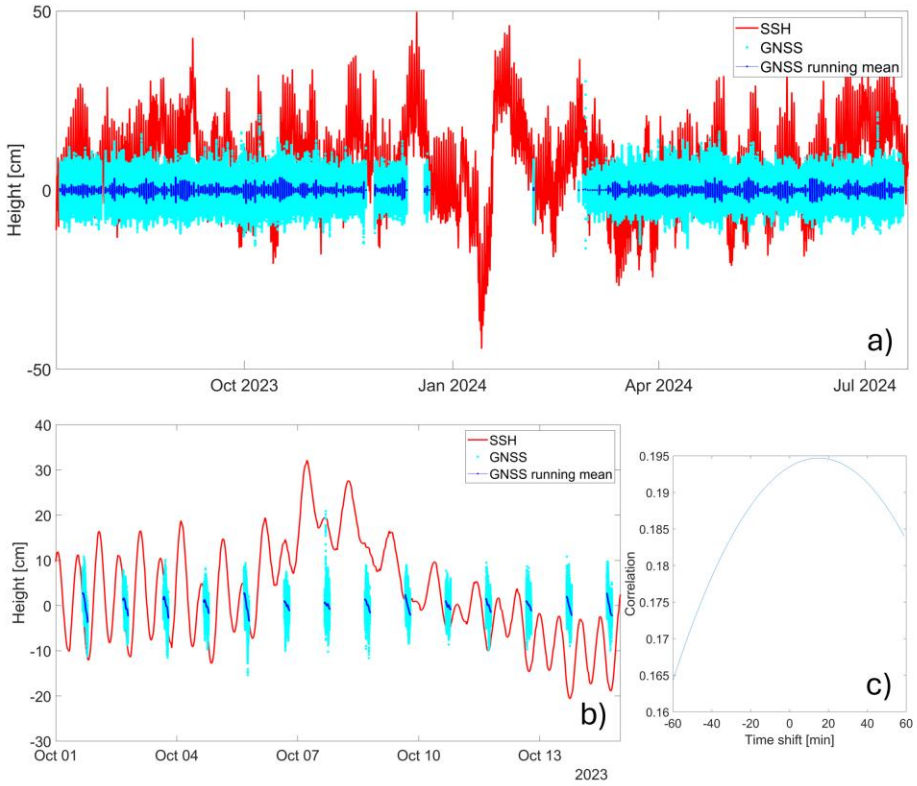

Figure 6AR: Correlation analysis between SSH and GNSS records in the flexure zone: a) Time series of SSH and GNSS-derived surface heights; b) Zoom-in on the October records to demonstrate oscillations in the GNSS data; c) Correlation between SSH and GNSS (running mean) with respect to time shift.

Minor comments:

L14: Reword from "Changes at the boundary" to "Changes of the boundary" as the grounding line location generally serves as a proxy for stability considerations in numerical models.

We revised the sentence as follows:
"Observing and quantifying changes in the boundary where marine-terminating glaciers transition from grounded to floating ice, known as the grounding line, is critical for advancing our understanding of glacier stability."

While we agree that grounding-line position is particularly important for numerical modeling, we also intend to convey that not only positional changes are relevant, but also variations in glacier velocity and water intrusions behind pinning points (discussed in this manuscript), which can, in turn, lead to changes in the grounding-line position.

L15: Terminology. Reword here and throughout from "ice-flexure zone" to "tidal-flexure zone"

Thank you. We have revised the terminology and replaced "ice-flexure zone" with "tidal-flexure zone," since "tidal flexure" or "flexure" are more commonly used in combination with "zone" in

the literature. While terms such as "ice flexure" or "tidal ice flexure" are also used, they generally appear without "zone" (e.g., Brunt et al., 2010; Freer et al., 2023; Wallis et al., 2024).

L19: Terminology. Reword here and throughout from "Double Difference Interferometric SAR (DDInSAR)" to "Differential Interferometric SAR (DInSAR)". The word interferometric implies a (phase) difference between SAR images, the differential implies that two interferograms are being differenced. I know that DDInSAR can be found in the literature, but DInSAR is the modern terminology and the community strives to get rid of DDInSAR.

Thank you for the detailed clarifications. Yes, both versions of this term can be found in the literature. We have revised the terminology to adopt "DInSAR".

L23/24: Terminology. Reword here and throughout from "stable/unstable regime" to "steady/unsteady period". Stability of a glacier system is carefully defined in the ice-dynamics modeling community and we shouldn't use the term for other processes than MISI or MICI. Here, even if Milne Glacier experiences MISI, the analysis is concerned with the assumption of steady flow in DInSAR processing. In line with this, also reword "changes in glacier velocity were minimal" to "glacier flow was steady" and "more variable" to "unsteady". I also wonder if a single observation of an unsteady period warrants the classification as a "regime" or "phase". I suggest rewording these terms to "period".

We have revised the terminology to adopt "steady/unsteady period." However, we prefer to retain our original wording, for "changes in glacier velocity were minimal," rather than the suggested "glacier flow was steady," which would result in:
"The lowest error (<0.1 cm in the SAR line-of-sight) occurred during the 'steady period', when glacier flow was steady, with ascending RCM tracks at incidence angles below 30º."
We consider this formulation redundant and potentially misleading, as "steady glacier flow" may imply steady-state conditions in the glaciological sense, i.e., equivalence between ice mass input and output and also used by the modeling community (e.g., Sergienko, 2022), which is not the intended meaning in our case.

L32: Please replace the citation of the IPCC with original research in a discipline-specific journal like *The Cryosphere*.

The sentence and the citation were revised as follows:
"Rising atmospheric and oceanic temperatures can cause these glaciers to accelerate, leading to increased sea level rise and discharge of icebergs or ice islands into adjacent waters (Morlighem et al., 2019; Wood et al., 2021; Carnahan et al., 2022; Holmes et al., 2025)."

L38: Change "migrating with tides" to "migrating with tides over short time scales (Freer et al., 2023)"

The sentence was revised as follows:
"The grounding line exhibits dynamic behaviour, migrating with tides over short time scales (Freer et al., 2023) and advancing or retreating in response to changes in glacier dynamics over the long term (Milillo et al., 2022; Chartrand et al., 2024)."

L41: Change “DDInSAR” here and throughout to “DInSAR”. This means that “DSSH” can later be more intuitively compared to “DInSAR”.

The term and its abbreviation have been updated throughout the manuscript.

L43: “4 days” please compare to other often used SAR satellites like Sentinel-1, TerraSAR-X, COSMO, etc. Is this a dedicated mission, if so, please add this piece of information.

We revised the sentence and added additional information to compare RCM with other operational missions explored in the literature:

“The satellite-based Differential Interferometric Synthetic Aperture Radar (DInSAR) method has been proven to be highly effective for accurate monitoring of grounding-line migration, providing high temporal (1-6 days) and spatial (1 m to a few metres) resolution imagery, along with consistent multi-temporal coverage over large areas ranging from tens to several hundreds of kilometers (Rignot et al., 2011; Milillo et al., 2017). Among the currently operational SAR missions explored for DInSAR grounding-line applications, the RADARSAT Constellation Mission (RCM, C-band) has a 4-day acquisition cycle (Antropova et al., 2024; Gadi et al., 2025). This is comparable to COSMO-SkyMed (X-band) allowing 1 to 4 day revisits (Milillo et al., 2022; Rignot et al., 2024), and shorter than Sentinel-1 (C-band) with 6 to 12 day revisits (shorter with the A+B or A+C constellations) (Ramanath et al., 2025; Wild et al., 2025), TerraSAR-X (X-band) providing 11-day revisit (shorter with TanDEM-X) (Wild et al., 2018; Wild et al., 2025), and ALOS PALSAR (L-band) with 46-day revisit (Rignot et al., 2011). The relatively short revisit time of RCM enables high phase coherence, while its C-band wavelength provides sensitivity to small vertical displacements, allowing reliable DInSAR measurements for grounding-line monitoring.”

L43: Kim et al. 2024 use a terrestrial radar system, while the present study is about a space-borne system. Please clarify the difference or replace this reference with other DInSAR based studies of which there are many other relevant ones.

Thank you. Yes, this terrestrial radar-based DInSAR study was cited in the context of sub-daily acquisitions. We decided to focus on satellite-based SAR missions only and revised the text accordingly (as stated in our response above); the citation “Kim et al., 2024” was removed.

L46: Define “Hydrostatic line” here, as it is used later in the paper but I can’t remember to have seen its definition.

The sentence was revised as follows:

“The DInSAR method detects the ice flexure zone (FZ), where the glacier surface flexes with tides. This zone, also referred to as the grounding zone in some studies (e.g., Fricker et al., 2009; Freer et al., 2023), spans from the inland limit of tidal flexure (i.e., the hinge line) past the grounding line to the seaward limit of flexure (i.e., hydrostatic equilibrium line), where hydrostatic equilibrium is reached and ice tongue becomes completely buoyant.”

L50: Terminology. Reword here and throughout “FZ span” to “tidal-flexure zone”, and “GZ span” to “grounding zone” and refer to their width.

We replaced the abbreviations FZ and GZ with their full terms, although abbreviations seem to be acceptable in The Cryosphere (e.g., use of ‘GL’ for grounding line by Le Meur et al., 2014). We note that the “tidal-flexure zone” is equivalent to the “flexure zone” in the context of this manuscript, as defined in the text and consistent with recent studies.
We acknowledge that “grounding zone width” is more commonly used in the literature; however, some argue that this terminology can be misleading, since the distance is measured along the glacier flow rather than across it. We believe that terms such as along glacier “extent” or “span” could be more precise. Nevertheless, we adopt the term “width” for both the tidal-flexure zone and the grounding zone, to remain consistent with its frequent usage in the literature. We also note that “FZ span” is equivalent to FZ width measured along the glacier from a DInSAR result, while GZ width is calculated based on all available DInSAR results.

L55: Causes of complexity. The most relevant citations for the present study are Rack et al., 2017 and Wild et al., 2018.

Thank you, we added these citations:
“Recent DInSAR-based studies highlighted the complexity of grounding line migration with tidal cycles and explored the causes of this complexity, including glacier geometry, underlying bed type, subglacial hydrology, and sea water intrusions (e.g., Mohajerani et al., 2021; Ciracì et al., 2023, Rignot et al., 2024; Kim et al., 2024), as well as the contributions of compressional and tensional strain components induced by ice-surface bending to the DInSAR signal (Rack et al., 2017; Wild et al., 2018).”

L65: What “model datasets” ? It sets up the expectation of the reader to see some form of tidal-flexure modeling. Coming back to this after reading the paper, I think this is only GEM, right ? I think to warrant the “model datasets” here requires to perform the analysis at least with and without the GEM-derived IBE, in comparison with the GNSS analysis.

We revised the following sentences in the Introduction section to better clarify our datasets:
“Our study explores intra-annual changes in the Milne Glacier FZ based on a combination of RCM DInSAR-derived results, in-situ and simulated datasets, and a numerical weather prediction model output.”
“Examine the relationship between DInSAR-derived ice-surface vertical displacement and displacement of sea surface height (DSSH), computed from simulated tides and modeled atmospheric pressure outputs together with in situ atmospheric pressure records.”

L67: Perfect location to add a statement about the quantification of the steady-flow assumption during times when it is clearly violated. I believe this should be the real focus of the manuscript.

Thank you, we refined this objective in the Introduction section as follows:

"We further assess this correlation across the four SAR orbits with respect to the compressional and tensional strains caused by ice-surface bending in the FZ during two velocity periods:

a) a steady period, when the in situ-measured Milne Glacier velocity did not change appreciably during winter and the DInSAR assumption of invariant velocities was met; and

b) an unsteady period, when velocity changes were evident, the glacier decelerated after a velocity peak in summer, and the DInSAR assumption of invariant velocities was violated."

L78: Add information about the tidal range and tidal regime. Is it a diurnal or semi-diurnal tide ? How long is the spring-neap-spring tidal cycle ? The introduction of the epishelf lake is of course interesting, but the space should be used for more relevant information to the paper, such as what is known about Milne Glacier's velocity variability, and how it motivates a hypothesis (I suggest to use the known velocity variability as a motivation to analyse how different viewing geometries are affected by horizontal flow variability).

We revised the "Study Site" section, removing some details about the epishelf lake formation and adding information related to tidal processes:

"The intact floating ice tongue, located deep within Milne Fiord, is protected from the impact of sea ice drifts originating from the northeast by down-fjord ice features and by Cape Egerton to the east (Mortimer et al., 2012). The floating ice tongue experiences moderate stresses due to tidal bending. Milne Fiord is characterized by a semi-diurnal tidal regime with a relatively small tidal range, spanning from –20 cm to 21 cm over the observation period of this study, and a 14.8-day spring-neap-spring cycle. However, atmospheric pressure also plays an important role in modulating sea surface height in the fjord (Wunsch & Stammer, 1997; Padman et al., 2003), further affecting the displacement of the ice tongue and increasing the stresses it experiences.
The grounded part of the glacier just above the ice tongue exhibited notable velocity fluctuations over the past decades. Ice velocity decreased from ~190 m yr^{-1} to ~100 m yr^{-1} between the 1990s and 2005 (Millan et al., 2017), increased to 120 - 140 m yr^{-1} in 2010, slowed down again to 80 - 100 m yr^{-1} from 2011 to 2015, and then accelerated to 140 - 160 m yr^{-1} between 2016 and 2020 (Van Wychen et al., 2020)."

L106: How many km upstream is the mentioned prograde bed slope ? How many years of average grounding-line retreat will it take to be reached ?

We added the suggested details as follows:

"This positive feedback loop may be underway currently and is expected to persist until the grounding line reaches a prograde bed slope roughly 1 km upglacier, which, based on the glacier's average retreat rate from 2011 to 2023, could occur in about 11 years. Reaching this slope will help stabilize the glacier and inhibit further recession of its grounding line."

L108: Data and methods. Please add sub-section titles such as "Differential InSAR processing", "In-situ data", "Tide modeling", "Uncertainty analysis", "Grounding-zone width modeling", etc…

We distinguished the following preliminary subsections and revised their order based on our analysis:

2.2.1 Processing of SAR data
2.2.2 Analysis of tides
2.2.3 Analysis of velocity and ice surface bending components in the SAR signal from four RCM orbits
2.2.4 Reconstruction of ice surface heights time series
2.2.5 Analysis of flexure and grounding zones parameters

L111: A 10m spatial resolution is stated in the abstract, here 5m native resolution and the table shows about 2.5m raw pixel size. I know how these are affected by multi-looking and the topographic correction, so please describe these processing steps in more detail and state the chosen variables, which is also a great motivation to acquire a higher-resolution DEM to not lose any information in RCM.

We provided additional details on the RCM SAR products and our choice of spatial resolution for the final DInSAR results:

"We used RCM single look complex (SLC) images with HH polarization, acquired in 'High Resolution 5m Mode' (MDA, 2021) from different orbits during 2023–2024 (Table 1). This mode has a nominal resolution (i.e., theoretical resolution, which is based on radar system parameters) of 5 m and a swath width of 30 km. The native SLC pixel spacing is 1.4–2.8 m in the range direction and 2.4–2.8 m in the azimuth direction (Table 1)."
"Interferograms were computed for each pair of RCM data acquisitions with a 4-day interval. During processing, we applied 3 × 3 multilooking to reduce speckle, improve the signal-to-noise ratio and interferometric coherence, and reduce file sizes to facilitate phase unwrapping. After multilooking, the effective ground pixel spacing was approximately 9–10 m. Topographic phase removal and terrain correction were performed using the 10 m ArcticDEM (Porter et al., 2023). The minimum-cost flow phase unwrapping algorithm described by Costantini (1998) was used for the interferogram unwrapping. During the initial unwrapping, the processing software automatically selected an arbitrary stable reference area. Then, double difference results were calculated at 10 m resolution (i.e., the final spatial resolution of DInSAR images used for flexure zone delineations) for interferogram pairs and the corresponding unwrapped results represented by three consecutive data acquisitions (over 8 days) or four data acquisitions (over ≥12 days) if there was a gap between data acquisitions.".

RCM modes descriptions by MDA, (2021) can be found at:
https://download-telecharger.services.geo.ca/pub/csa_asc/Space-technology_Technologie-spatiale/radarsat_constellation_mission_plan/RCM-SP-52-9092_Product_Spec_1-15_Public.pdf

L115: What seems to me the most important information is that orbit 9 has twice as large incidence angle as the other orbits. This should be better visible in the table and the description of the RCM data, which sets the paper up nicely for developing the unsteady-flow quantification or even the bending-effect hypotheses outlined in the major comments.

We highlighted this information in the table by adding the following footnote:

"[2] The incidence angle of orbit 9 is 1.4–2 times greater than that of orbits 43, 58, and 103."

Also, the following information was added to "2.2.3 Analysis of velocity and ice surface bending components in the SAR signal from four RCM orbits" section:

"Inputs from unsteady velocity between SAR data acquisitions and ice surface bending contributions to the SAR signal were examined among four RCM orbits. The orbits were characterized by varying incidence angles used for line-of-sight error calculations (Table 1.1): three of the orbits had similar angles of 20.3°, 21.5°, and 27.5° for orbits 43, 53, and 103, respectively, while orbit 09 had a much higher incidence angle of 39.5°".

L121: reword to "effect of steady glacier flow".

We added "steady" to the sentence:

"This method reveals the surface displacement of the floating ice tongue along the SAR line-of-sight, by removing the effect of steady glacier flow, through differencing two consecutive interferograms, under the assumption that the glacier velocity remains constant between SAR acquisitions."

L122: hydrostatic equilibrium line is not defined yet. Terminology. Also, please avoid confusion with the abbreviation of hinge line. Commonly HL denotes the hydrostatic line, and hinge line is spelled out.

The hydrostatic equilibrium line is now defined in the Introduction (as per the comment above). The "hinge line" term is spelled out in the manuscript text and represented by the "HL" notation only in Fig. 9a, which was removed.

L123: Terminology. Reword to "landward and seaward limits of the tidal-flexure pattern". The boundaries normally refer to already delineated GL and HL. Also, reword "glacier flexure" to "tidal flexure". I understand that the main contributor to "glacier flexure" here is the IBE, but the geophysical process is commonly called tidal flexure, and the IBE is one contributor (aside ocean tides and tidal loading on the Earth's crust, which is neglected here, right ?).

We revised the sentence as follows:
"The hinge line and the hydrostatic equilibrium line are then manually delineated by examining the landward and seaward limits of the fringe pattern in the DInSAR results representing the flexure zone."
We replaced "glacier flexure" with "flexure zone." We consider the term "flexure zone," equivalent to "tidal-flexure zone," to be appropriate, as it is defined in the Introduction and is widely accepted in the literature. Indeed, we believe that the use of "flexure zone" is more intuitive, as it allows encompassing multiple driving factors (e.g., atmospheric pressure, ice thickness and stiffness, glacier geometry, and the presence of pinning points that can redistribute stresses and shape the flexure zone), rather than referring solely to tidal forcing.
We also added the clarification about ocean tide load in "2.2.2 Analysis of tides"' section:

"Simulated tide heights were corrected for the inverse barometer effect (IBE) (Wunsch & Stammer, 1997; Padman et al., 2003), while ocean tide loading on the Earth's crust was neglected, as it has a relatively minor impact (Wild et al., 2025)."

L126: To better distinguish between DInSAR images (the double-difference result) and times of single tide snapshots, please reword here and throughout to "three or four consecutive SAR data acquisitions" or "SAR scenes" to underline the snapshot character of the SAR data.

We replaced the corresponding entries with "SAR data acquisitions."

L129/130: First and only mention of phase-loss in lateral margins. Please add how ice-flow rotation leads to loss of coherence required for interferometry. Also, please read Wild et al., 2025 how weakening of ice properties in these zones affect stiffness and thus the flexural response of the entire glacier. This signal provides an exciting avenue for further research on bulk ice stiffness and buttressing. This section also lacks information of phase unwrapping and the coordinate used as a reference, which is also not shown in the figures.

The suggested information was added to the text as follows:

"The western and eastern flexure-zone boundaries were often affected by noise. These noisy areas, with a loss of interferometric coherence, typically occurs due to strong velocity gradients, shear, ice deformation, and rotation as glacier velocities decrease from the centre toward the lateral margins as a result of lateral drag (Forster et al., 1999; Mannerfelt et al., 2025). These processes contribute to ice weakening and a reduction in stiffness (e.g., a fivefold reduction in Young's modulus reported by Wild et al., 2025) in the lateral shear margins. This interpretation is supported by our in situ observations and high-resolution imagery demonstrating extensive crevassing in this zone, particularly along the western margin, where a tributary glacier further enhances these processes. The resulting loss of coherence in the flexure-zone's western and eastern boundaries prevented their reliable delineation and the use of the entire area of the FZ flexure zone for our analysis."

We added the following information about phase unwrapping:

"The interferogram unwrapping was performed using the minimum-cost flow phase unwrapping algorithm described by Costantini (1998). During the initial unwrapping, the processing software automatically selected an arbitrary stable reference area."

L142: How were phase discontinuities corrected ? Only along the transects ? This and the mention of division by cosine of the incidence angle to get displacement should be moved to a dedicated DInSAR processing subsection in the methods.

Yes, the phase discontinuities were corrected along the transects with known bed geometry. We added clarifying details to the text and moved it to the DInSAR processing description section:

"The final calibration of the SAR line-of-sight displacement was conducted along the three transects (Fig. 1) using an automated script. Values were divided by the cosine of the incidence

angle, additionally calibrated to the mean grounded ice surface value for orbit 9, and then corrected for phase jumps exceeding 2 cm (i.e., more conservative than half of the RCM C-band wavelength)."

L154: The correct references for the importance of atmospheric pressure are Rignot et al., 2000 and Padman et al., 2003.

Thank you. We have replaced the citation with these two earlier studies.

L156: t-tide analysis. Please quantify how accurately the t-tide prediction replicates the input data, and how well it fits to an independent tidal model (such as Gr1kmTM). How do these uncertainties affect the results ? Is there a time delay between modeled tides and GNSS displacement ?

Our T_TIDE simulations were conducted based on 'a 10-month in situ pressure record from an RBR Duet datalogger moored at ~10 m depth in a lateral bay off the west side of Milne Fiord (Antropova et al., 2024)', rather than on GNSS ice surface displacement data measured on a freely floating ice tongue. The manuscript text was revised to explain this directly, rather than referring to Antropova et al. (2024). In this study, GNSS records were primarily used to investigate displacement due to ice flow in the grounding zone, where the ice was not freely floating; therefore, these records were not suitable for tidal simulations. We computed the requested statistics using our pressure-record observations and consider that the question of a time delay is not relevant to our dataset.
The comparison of detrended 2016-2017 in situ pressure-based tide records with tides computed using T_TIDE and Gr1kmTM (Fig. 7AR) shows correlation of 0.83 vs. 0.73 and RMSE values of 4.7 cm vs. 5.9 cm, for T_TIDE vs. Gr1kmTM, respectively. Therefore, T_TIDE is more accurate than Gr1kmTM as it shows better agreement with the observed tides than Gr1kmTM.

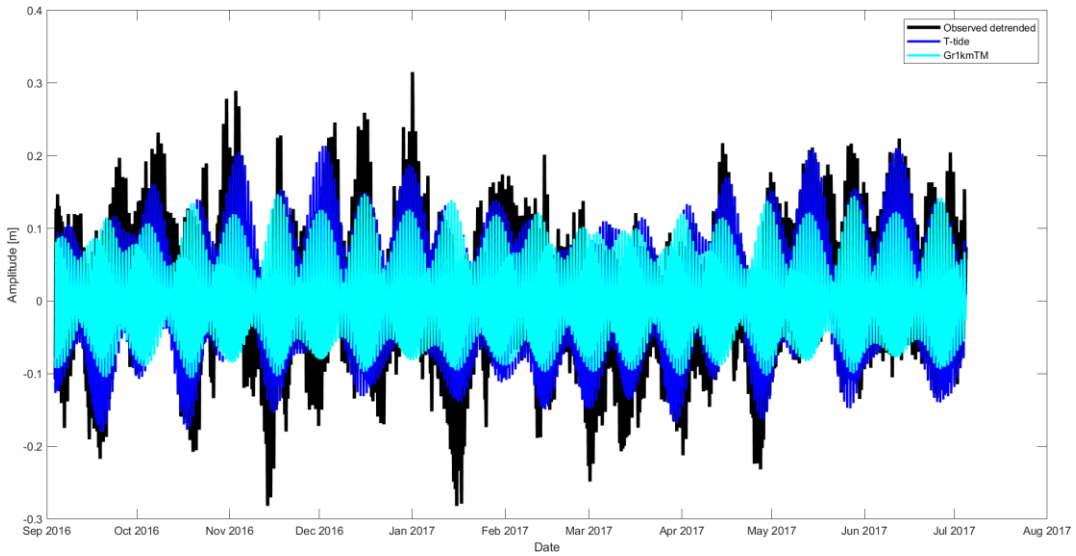

Figure 7AR: In-situ pressure-based tide records and simulated tides using T-tide algorithm and Gr1kmTM model.

We also added to the manuscript a comparison of an independent tide data sample (i.e., not used as an input for the tide simulations) collected in July 2023 against the simulated tides, with GEM-

based IBE included, to the Appendix. Based on this comparison, which represents the observed conditions better than the detrending approach above and falls within our observation period, the correlation was 0.96 vs. 0.93 and the RMSE was 3.4 cm vs. 4.6 cm for the T_TIDE- and Gr1kmTM -based outputs, respectively. Thus, T_TIDE demonstrated better agreement with the observed tides than GR1kmTM.
The following text was added to the manuscript:

"The SSH computed using T_TIDE showed a higher correlation (0.96 vs. 0.93) and lower RMSE (3.4 cm vs. 4.6 cm) than the independent tidal model GR1kmTM (Howard and Padman, 2021) when compared with repeated in situ tidal observations collected in July 2023" (Fig. 8AR).

The following figure was added to the Appendix:

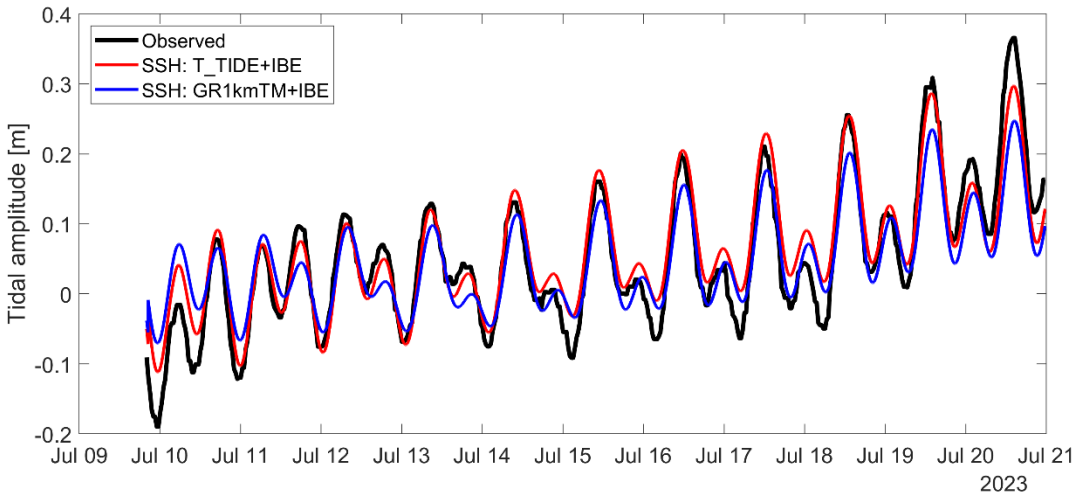

Figure 8AR: Observed tide records measured in situ in July 2023 (black) and computed sea surface heights (SSH) using the T-tide algorithm and the Gr1kmTM model, with IBE added (red and blue, respectively). The correlation between the observed and computed SSH based on the T_TIDE and Gr1kmTM is 0.96 vs. 0.93 and the RMSE is 3.4 cm vs. 4.6 cm, respectively.

L157: Reword "corrected" to "added to" the IBE, since atmospheric pressure variations are a contributor to the tidal forcing (sum of ocean tides, load tides, and the IBE). Also, please add the conversion factor, was it 1cm drop for every positive anomaly of 1hPa ? Were pressure anomalies calculated over the entire time span, or over shorter chunks ?

The corresponding sentences were revised as follows:

"Simulated tide heights were corrected by adding the inverse barometer effect (IBE) (Wunsch & Stammer, 1997; Padman et al., 2003), while ocean tide loading on the Earth's crust was neglected, as it has a relatively minor impact (Wild et al., 2025). We used the atmospheric pressure data recorded by our in situ weather stations (Fig. 2 c) to calculate the IBE over the entire observation period, assuming that a 1 hPa increase (decrease) in atmospheric pressure results in a 1 cm drop (rise) in sea level (Wunsch & Stammer, 1997; Padman et al., 2003). This correction was then added to the simulated tides to compute the sea surface height (SSH)."

L160: What's the temporal resolution of GEM ? Fig. 2c indicates it is lower resolution than the AWS data. Was the AWS pressure record low-pass filtered to a common cutoff frequency before any gaps were filled to account for any differences in temporal resolution ?

The temporal resolution of GEM is 1 hour, whereas the temporal resolution of AWS is 30 minutes. We added information about time intervals to the corresponding section. Our tidal time series were simulated at a 1-minute interval in order to better match the acquisition times of the SAR data. The pressure records from AWS and GEM were used to calculate the IBE values, which were then linearly interpolated to a 1-minute interval and added to the tidal time series. The following clarifications were added to the manuscript:

"This correction was linearly interpolated to a 1-minite interval and then added to the simulated tides to compute the sea surface height (SSH)."

We also note that a gap in the AWS records occurred between July 9 and July 21, 2023, during which no coherent DInSAR results were available for our analysis, and after July 22, 2024, when only one SAR triplet was acquired in September. Therefore, the GEM-based correction corresponds to only one DInSAR result in our analysis.

L162: Please quantify "good agreement" between GEM and AWS data. For a direct comparison, the AWS records will need to be low-pass filtered with the cutoff frequency of GEM before any correlations and RMSE can be calculated.

The following information was added to the manuscript:
"In particular, the correlation between the GEM and in situ atmospheric pressure records used for IBE calculations was 0.96, with the RMSE of 3.6 hPa."

L163: Reword "DDInSAR result" to "DInSAR image" and also change to "SAR data acquisition" or "SAR scenes".

"SAR acquisition(s)" entries were replaced with "SAR data acquisition," as stated above.

L164: Reword "DDInSAR subtraction", which implies a triple difference to "DInSAR combinations", which I think is not meant here.

"DDInSAR" entries were replaced with "DInSAR," as stated above.

L165: Where along each profile is DInSAR-derived surface height taken ? Normally a "freely-floating area" is averaged over, but this reads as if the far left side of each profile was taken ? To minimize the effect of interferogram noise, I suggest averaging over everything larger than 47 km distance, or even better any DInSAR displacement beyond the delineated hydrostatic lines.

Yes, the DInSAR-derived surface heights was calculated as the mean values. We added the following clarifying information to the manuscript:

"We assessed the relationship between DSSH and DInSAR-derived surface height displacement of the freely floating ice tongue (i.e., mean values calculated from 44 km downfjord along the three transects in Fig. 1) based on the correlation coefficient, the root mean squared error (RMSE), and bias."

L171: DInSAR images contain information about the net sum of all tidal constituents (plus IBE and tidal loading) so fitting with a single constituent is physically invalid. Please refer to the methodology presented by Minchew et al., 2016 how to deal with apriori information on each sinusoid before the inversion, or employ an alpha map based approach for the unraveling to single tides.

We improved our initial least-squares fitting approach by including all tidal constituents (i.e., 59) computed using the T_TIDE algorithm and IBE. The coefficients of the harmonic components were computed using a regularized least-squares approach. Our results (Fig. RA3) above demonstrate RMSE of ~5 cm. Given that T_TIDE shows the correlation of 0.96 and the RMSE of 3.4 cm with our in situ tidal observations, the obtained RMSE of ~5 cm in our reconstruction analysis is reasonable.

L172: Please reword here and throughout from "SAR acquisitions" to "SAR data acquisitions" or "SAR scenes".

"SAR acquisition(s)" entries were replaced with "SAR data acquisition," as stated above.

L174-176: "We used SSH…" I do not follow this sentence, please rephrase and say what hypothesis is investigated and how it is done.

L174-176 were revised as follows:

"To explore the origin of the newly developed notch along the eastern margin, we tested the hypothesis that it appears in DInSAR images associated with SAR acquisitions during periods of high SSH, suggesting that seawater intrudes farther inland and results in ice ungrounding around a pinning point. We calculated the minimum and maximum SSH values, as well as the standard deviation, for each DInSAR result associated with three or four SAR data acquisitions. These values were then divided into two groups corresponding to: (1) DInSAR results without the notch and (2) DInSAR results with the newly developed notch present, to test whether SSH differs significantly between the groups."

L176: Reword "grounding-line delineations" with "tidal flexure zone delineations".

This sentence was revised as per the comment above, and the term "grounding-line delineations" was removed.

L180: Terminology: Reword "SAR observations" to "SAR data acquisitions" or "SAR scenes". The word observation normally refers to processed DInSAR images.

"SAR observations" was replaced with "SAR data acquisitions".

L183: Do the three hour GNSS acquisition period introduce a tidal bias in the derived mean daily velocity ?Is the error of 1.5 cm considered in the uncertainty analysis ?

The GNSS device was installed in the flexure zone; therefore, GNSS measurements (daily mean values for the stabilized GNSS position between 18:00 and 19:00 UTC) were also affected by tidal bending. SAR data for orbits 43, 58, and 103 were acquired approximately 1 hour after the GNSS records. Orbit 09 had a much larger timing lag relative to the GNSS observations and therefore captured a tidal signal different from that recorded by the GNSS.

SAR data acquisition times (UTC):
Orbit 43: 19:58:00;
Orbit 09: 13:19:00;
Orbit 58: 20:06:00;
Orbit 103: 20:30:00;

We added information about the timing of GNSS measurements and tidal bending to the manuscript.
We did not explicitly account for an error of 1.5 cm. Velocity was calculated through the change in distance relative to the previous GNSS position; assuming a similar positional error for each record, the error largely cancels out.

L190: Quantify "agreed well" with an RMSE. Looking at Fig. 2a this is only true for the steady periods but the agreement isn't that good during summer and into the unsteady period.

We note that SAR velocities were computed to support our GNSS-based velocities during the period of missing records, which corresponds to the period of good agreement. The following information was added:

"The missing GNSS records (10.5% of the total records within the analysed periods) at the end of the unsteady period and beginning of the steady period in 2024 were linearly interpolated from neighbouring observations. The interpolated values agreed within ±1 cm with SAR-derived velocities computed to support the missing GNSS records. The Milne Glacier velocity, averaged within 3x3 pixel window at the GNSS receiver location (Fig. 1), is shown in Fig. 2a."

In addition, SAR velocity is affected by speckle noise. While values tend to be more consistent and reliable when analyzed and spatially averaged over larger areas, point-based comparison, as in our case, is much more complicated due to noise, especially when melt processes affect the SAR signal. The figure demonstrates that the agreement is very good during the stable (cold) season. It is not surprising that summertime results demonstrate weaker agreement, as SAR data acquisitions are much sparser during this period, the SAR signal is affected by melt processes, and, likely, by much more pronounced glacier deformation due to ice flow acceleration.

L192: Reword from "effect of velocity" to "effect of velocity variability"

We added the word "variability".

L201: Please label “Purple Valley” in Fig. 1

The label was added.

L204: Reword “DDInSAR observations” to “SAR data acquisition times for four different orbits”.

We made the requested replacement.

L209: Please add the percentage of missing GNSS records of the total period of investigation.

“10.5% of the total records within the analysed periods” as per the comment above.

L211-218: Very nice. It would have been beneficial to also conduct this part of the error analysis with the SAR-derived velocity fields and analyze any spatial patterns of the steady flow assumption.

We believe that our approach, based on in situ GNSS measurements, is of interest to the broader community of The Cryosphere. Therefore, we retain the GNSS-based velocities in our analysis and consider a detailed analysis using SAR-derived velocities to be beyond the scope of this manuscript.

L236: Do the delineations of grounding-zone width need to be corrected for the “bending effect” to be comparable to the theoretical width determined by Tsai and Gudmundsson ? In other words, is this a model for neutral layer displacement ?

We infer that Tsai & Gudmundsson (2015) assumed negligible bending stresses for “sufficiently long” ice shelves. Likewise, Chen et al. (2023) and Mohajerani et al. (2021) neglected bending stresses, although they compared their DInSAR-derived results with the theoretical width predicted by Tsai & Gudmundsson (2015).
We added the following statements to better clarify that bending stresses were not considered here:

“This equation was derived by Tsai and Gudmundsson (2015) based on prograde bed geometry and was later applied to both retrograde and prograde bed geometries, assuming negligible bending stresses at the ice surface (e.g., Chen et al., 2023).”

Fig. 10 caption was revised as follows:

“The calculated width of the grounding zone (displayed in text) is about 22 to 74 times smaller than the DInSAR-derived grounding zone, which does not include correction for the bending effect (shown with red dashed lines).”

L240: reword “RCM images” to “SAR-data acquisitions" or “SAR scenes”.

We replaced “RCM images” with “RCM SAR scenes” here.

L245: This is not surprising, given that ice stiffness controls the width of the tidal-flexure zone.

This sentence was removed, as this part is covered in detail in the Discussion section

L254: Reword "during the last part of our intensive observation period" to " towards the end of the observation period".

The "toward the end of the observation period" replacement was done.

L263: Reword "atmospheric pressure" to "IBE" or "atmospheric pressure variability", which is what is causing this signal.

The "atmospheric pressure" was replaced with "IBE".

L267-269: "These correlations…" move to Discussion.

These sentences have been moved to the Discussion section.

L269-272: I think that one must add that the result of a double difference can have a larger absolute value than any of the individual values. So a 2.3 fold increase is essentially a measure of the non-linearity of the investigated process (a tiny change at the times of the SAR-data acquisitions will result in a much larger value in the DInSAR combination). So adding the IBE, which is known to dominate in areas with small tidal range, will greatly improve any correlation with DInSAR measurements on the freely-floating part. Therefore, I think that it is useful to report on how the IBE improves the correlation at Milne Glacier, but it shouldn't be a main finding with a dedicated Figure in the main text. I suggest moving Fig.4 to the Appendix or SI, and cut back on the interpretation in the main text.

Thank you. We retained only panels for correlation between SSH and DInSAR displacement in the manuscript and moved the other panels to the Appendix. We also revised the manuscript to tone down the discussion of IBE.

L272: Great that correlations improved after the IBE, but the RMSE is still huge when compared to the signal, about 15 cm of 50 cm DSSH. Please refer to the "tide-deflection ratio" approach outlined above on how to further minimize the RMSE to be within interferogram noise (<1cm).

Thank you for your suggestion. However, our study aims to explore the "standard" DInSAR method and its assumption of steady flow velocity. Therefore, we consider reporting these results to be a necessary step in our analysis. As reported above, the correlation between the observed and computed SSH based on T_TIDE was 0.96, and the RMSE was 3.4 cm. We also note that our RMSE is comparable to values reported in recent studies using the same method (e.g., inferred from Fig. 2c in Chen et al., 2023, and Fig. 3b in Rignot et al., 2024). Therefore, we consider our RMSE values to be reasonable for the method used in this study.
In addition, we emphasize that our GNSS records do not provide reliable information on ice surface displacement for the freely floating ice tongue, and thus we do not have the opportunity to use them for validation of the tidal predictions as done by Wild et al. (2019). We prefer to retain our

"standard" DInSAR approach and consider the "tide-deflection ratio" approach to be outside the scope of the current manuscript. However, we would be happy to share our interferograms and other available processed datasets with interested members of the glaciological community for further exploration of these processes using the "tide-deflection ratio" and other approaches.

L301: I don't quite agree with this interpretation (which also needs to be moved to the Discussion). The width of the flexure zone is independent of DSSH and only determined by ice stiffness. Also, the higher the DSSH, the more pronounced the spurious surface movement by the bending effect and thus the grounding-zone width.

We agree that ice stiffness controls the width of the flexure zone; however, pinning points can influence stress distribution, flow variability, and the apparent stiffness of the glacier system.
We moved the revised clarifications in the Discussion section:

"Previous studies have shown that the presence of pinning points affects lateral and basal shear stresses, producing upstream compression and downstream tension, which in turn influence flow variability and the apparent stiffness of the system (Robel et al., 2017; Still & Hulbe, 2021). Moreover, both observed pinning points are located within a lateral shear zone, which is associated with reduced ice stiffness (Wild et al., 2025). These processes may have contributed to the grounding-line retreat behind the pinning points and to the observed shape of the flexure zone."

L304-309: Nice quantification of the steady-flow assumption, which is the strength of the paper.

Thank you.

L314/315: Is this surprising ? Rather start this paragraph with why one would want to look at individual orbits and say that different incidence angles are more or less sensitive to horizontal flow variability.

No, it is not. We added the following sentence for a smoother transition:

"The sensitivity of DInSAR results to vertical and horizontal motion components depends on the incidence angle and look geometry (e.g., Rocca et al., 2010, Hu et al., 2014). Therefore, our results were analysed by orbit (Fig. 8)."

L320: The different sensitivity of different orbits is interesting and additional evidence that the bending effect is at play. This signal should ideally be explored for a more glaciological research question.

We added the additional analysis of contributions due to bending to our analysis (Fig. 2AR).

L330: Is this a typo ? Orbit 43 here should be orbit 09, right ?

Thank you; this was a typo and has been corrected to orbit 09.

L331: Replace “different viewing geometry” to “higher sensitivity to horizontal displacement and variability thereof.”

We revised the sentence as follows:
“Nevertheless, orbit 09 demonstrated higher correlation between DInSAR-derived displacements and DSSH for unsteady than steady period, which we attribute to its higher sensitivity to horizontal displacement and, consequently to velocity variability as well as ice extension and compression due to tidal bending.”

L333-346: I think this paragraph is speculative and the argumentation is invalid for the reasons outlined above and should therefore be removed. At a minimum, it should be moved from the results section to the Discussion section. The part talking about grounding-zone width (here distance between HL and point A) requires a dedicated investigation of the tidal forcing at the times of SAR data acquisition, which are here presented in their DInSAR combinations.
Similar to the width of the tidal-flexure zone (here Flexure zone span) and differential tidal displacement, where a linear regression over all the data seems physically unmotivated. The trends look statistically insignificant. I think this also presents either biases during the times of SAR-data acquisition or a temporal signal (which then can be linked to the emergence of new pinning points).

As per our response to the major comments, Figure 9 was removed, and information about flexure zone width and distance to the hinge line is now presented in a table. Our discussion was revised with respect to ice thickness, stiffness, viscoelastic response to tidal flexure, and emerging pinning points.

L351-367: This reads all like Discussion and should be moved out of the results section.

This section was revised. The manuscript text reporting values for the grounding zone width, the calculated theoretical grounding zone width, and the locations of bed rises along the transects was retained here. This text presents our results based on Fig. 10 and, therefore, we believe it should remain close to the figure. Text providing interpretations was moved to the Discussion.

L355: Wait, I thought the observations are not aligned with the theory by Tsai and Gudmundsson ? What did I miss ?

We never claimed that the observations are inconsistent with Tsai’s theory regarding the idea that the widest grounding zone occurs over the shallowest bed slope, and the steepest bed slope corresponds to the narrowest grounding zone (i.e., the expected direction of the relationship). The only discrepancy between the theory and the observations lies in the magnitude of the observed versus predicted values. We added the following clarifications:

“This pattern is aligned with the theory (Tsai & Gudmundsson, 2015) and literature (e.g., Rignot et al., 2024) in term s of the expected direction of the relationship.”

L374: Here we switch from m/d to m/yr. Please choose one unit throughout the manuscript (text and figures) so velocities can be easier compared between satellite and GNSS.

Thank you for the suggestion, but we prefer to use the m yr^{-1} notation in this section because it facilitates comparison with previous studies cited in the Study site description as well as comparison with grounding-zone and flexure-zone widths observed during the SAR data acquisition period. As clarified above, the daily velocities shown in Fig. 2 were used solely to support our daily GNSS observations.
We added the following clarifying sentence:

"To provide context for the observed grounding-zone and flexure-zone widths with respect to changes in glacier velocities, and to allow direct comparison with previously reported annual velocities (Millan et al., 2017; Van Wychen et al., 2020), we present velocities in annual notation in Fig. 11."

L377: A 2.7 fold increase between flexure-zone and grounded glacier speeds. This is more than the temporal acceleration observed in the GNSS data (eye-balled from Fig. 2a about 2.1 fold). Taken together, these observations indicate temporal variability of longitudinal strain rates. Was this signal investigated with respect to the emergence of new pinning points and short-term variability in buttressing strength? This provides another exciting avenue for this manuscript as spatial patterns could also be investigated with the data at hand.

We do not think so, as the GNSS data show a similar acceleration: the highest velocity peak was 1.09 m d^{-1}, while the steady-season velocity was about 0.4 m d^{-1}, corresponding to the same ~2.7-fold increase. Based on our GNSS records from 2019, 2024, and 2025, acceleration to 1.0 – 1.2 m d^{-1} is typical of the July velocity peak.

L386: Typo. "Fig. 11a" should be "Fig. 11c", right ? Also, the claim about larger ice discharge in the west requires calculation using the ice thicknesses shown in Fig. 10 and surface velocities.

Yes, thank you, the typo was corrected.
The following calculations were added to support the statement:

"The widest grounding zone along the western transect of the glacier was associated with the highest velocity of 166.4 m yr^{-1}, averaged over a year and across the observed grounding zone width (Fig. 11 c), and the thickest ice (mean value of 225.6 m, Fig. 10 d). This section discharged approximately 37 540 m^3 yr^{-1} of ice along a 1 m-wide flow line. The narrower and thinner grounding zones along the eastern and central transects, with mean thicknesses of 210.0 m and 200.5 m (Fig. 10 b, c), were associated with slower average velocities of 144.6 m yr^{-1} and 159.8 m yr^{-1} (Fig. 11 a, b), discharged approximately 30 366 m^3 yr^{-1} and 32 040 m^3 yr^{-1}, respectively."

L.387: Typo. "Fig. 11 b,c" should be "Fig. a,b", right ?

Yes, thank you, the typo was corrected.

Discussion: I found this section underwhelming as it's largely a summary of the presented results, without a clear evaluation of a glaciological hypothesis. I provided a few different avenues above and hope that depending on the target journal, this section will be reworked with either a remote-sensing focus or glaciological focus.

We revised the Discussion section, in particular, added discussion of the suggested bending effect to provide more detail on the remote-sensing aspects of the explored glaciological processes.

L400: Reword to “atmospheric pressure variability”

“Variability” was added to the phrase “atmospheric pressure.”

L410: Reword “pinning points drastically affected” to “pinning points control”

The suggested replacement was done.

L421: I suggest starting this paragraph with how DInSAR assumes steady flow to isolate the differential vertical component commonly referred to as a fringe pattern delineating the tidal-flexure zone. Then state how the present study quantifies this assumption with available GNSS data. The difference for different orbits then depends on the sensitivity to horizontal flow variability, which should be investigated with the available SAR-derived velocity fields.

Thank you, this part was revised as follows:

“This study is based on a commonly used DInSAR approach, which assumes steady glacier flow between SAR data acquisitions so that it can be isolated through interferogram differencing to reveal the vertical component of displacement due to tidal flexure. We examine the validity of this assumption by quantifying the SAR line-of-sight error caused by velocity variability using available in situ GNSS records. We also assess SAR line-of-sight errors resulting from ice stretching and compression associated with tidal bending. Furthermore, analysis of these results with respect to four RCM orbits with different incidence angles, and both ascending and descending passes - thus different sensitivities to horizontal flow variability - provides insights about the robustness of DInSAR flexure-zone delineations.”

L429: Typo. “39.6 deg” is “39.5 deg” in Tab. 1

Thank you, the typo was corrected.

L431: Replace "viewing geometry” to “sensitivity to horizontal flow variability”

The suggested replacement was done.

L435: Regarding the loss of coherence. Did you try to mask only ice-covered areas when matching slcs (the step before calculating interferograms). ? I found that this often greatly increases coherence compared to offset fitting the entire scene.

We did not apply masking of only ice-covered areas during SLC matching. Our interferograms have very short temporal baselines (a few days), and overall coherence across the scenes is generally high. The main areas of coherence loss correspond to zones of very rapid ice motion/deformation, where phase decorrelation occurs due to physical displacement between

acquisitions. In such cases, the loss of coherence is primarily driven by glacier dynamics and cannot be significantly improved through alternative coregistration strategies such as masking during offset estimation.

L437: Why are more in-situ velocity observations required ? I understood that the beginning of this paragraph that even though the velocity variability is large, the spurious signal in DInSAR issmall compared to the tidal forcing. I would have appreciated a statement how well only using SAR-derived velocity fields from speckle tracking can be used for estimating the spatial patterns of the steady flow assumption.

Thank you. We revised the sentence (please see below) to highlight the importance of using SAR-derived 3D/2D velocity fields. However, as mentioned above, we would like to retain our in situ GNSS analysis and consider the suggested only SAR-derived velocity analysis outside the scope of the current manuscript.

"With the increasing number of SAR observations, larger SAR datasets can be used to compute 3 D velocities (e.g., Samsonov et al., 2021), which when supported by reliable in situ tidal observations, will help to further investigate and quantify how the flexure-zone delineation is affected by the SAR viewing geometry with respect to changes in glacier velocity and bending."

L443: I think this is the bending effect, it's just more pronounced if the background flow is elevated. Another motivation for using the 2D velocity fields for a detailed analysis.

We agree that 2D or 3D velocity fields can provide additional information that may be useful for a more detailed analysis in the future. However, the precision of SAR offset tracking is typically on the order of about 1/10–1/20 of the pixel size. For our data, with a pixel spacing of ~2.5 m, this corresponds to approximately 0.1–0.25 m, which is about an order of magnitude lower than the precision achievable with InSAR.

L450: This sentence is quite speculative as the observations only show that the grounding line has retreated and acceleration is non-linear, but not that it's a runaway effect (which would require a numerical model of viscous ice-dynamics).

We revised the sentence as follows:

"This study documented glacier acceleration, which was preceded by grounding-line retreat, suggesting that this glacier, currently resting on a retrograde slope, is prone to marine ice-sheet instability."

L494: I want to encourage the authors to perform the suggested further investigation of viewing geometry.

The suggested bending analysis has been added to the manuscript.

Data availability:

I understand that raw data are often subject to license agreements and can therefore not be published, but how about the processed InSAR and DInSAR images ? I want to encourage the authors to provide them (together with the datetimes of the corresponding SAR scenes) to the scientific community.

We revised the text as follows to better clarify the data availability:

"The authors do not have permission to share raw RCM data, but it can be accessed by registering a vetted user account (https://www.asc-csa.gc.ca/eng/satellites/radarsat/access-to-data/about.asp). InSAR results, as well as other field, simulated, and modeled data used in this study, are available upon request. The IceBridge airborne radar data (IceBridge MCoRDS L2 Ice Thickness, Version 1 [IRMCR2_20140401_03], https://doi.org/10.5067/GDQ0CUCVTE2Q) are freely available at https://nsidc.org/data/irmcr2/versions/1."

Where is the IceBridge data available. Please provide a link and DOI.

We added details as per the comment above. This information is also included in the Acknowledgements and References sections.

The modern standard is to provide field-data sets to the scientific community through an online provider (PANGEA, USAP-DC, NSIDC, etc) about 2 years after they've been acquired. And not by request to the corresponding author.

Thank you for your suggestion. As of now we will be happy to share our datasets by request to provide additional clarifications. In the future, we will consider preparing our datasets for publishing online.

References:
Unify the formatting. Schoof, 2007 seems missing.

Thank you, Schoof (2007) was added to the list. We revised the formatting of references.

Figures

Figure 1:
I suggest adding two panels with the mean velocity fields over the steady and unsteady periods. Or the steady one, with the second showing the spatial variability of percentage acceleration during the unsteady phase. Also, add the extent of panel b to panel a. And the location of GNSS and the phase unwrapping point to panel b. Two arrows with flight direction and azimuth of the different orbits might also be useful to estimate the sensitivity to horizontal flow variability.

Thank you for the suggestions. We prefer not to include SAR-derived velocity fields, as our error analysis of DInSAR results is interpreted with respect to in situ GNSS observations. The extent of panel b has been added to panel a. We also added GNSS locations throughout the year to panel b; these locations were already present on panel a. Details about the SAR viewing geometry (i.e., pass, incidence angle, and track angle represented as azimuth clockwise from True North) are

presented in Table 1; therefore, we prefer not to repeat them here to avoid overcrowding of the introductory figure.

Figure 2:
Panel (a): What is going on with the SAR-derived velocity spike in 2024-01-02 ? It seems to overlap with an increase in air temperature - is this a real signal ?

We believe this is likely a real signal because: 1) it coincided with the air temperature rise, as you mentioned; 2) the spike was observed at other nearby locations (i.e., 3×3 pixel windows) and also associated with acceleration in Fig.11; 3) our second GNSS, located ~15 km up-glacier from the grounding zone, also recorded a small jump at this time (i.e., circled in Fig. 9AR below). Unfortunately, our GNSS located in the grounding zone stopped recording at this time, and we do not have any other solid confirmations; therefore, we prefer to avoid speculating about this signal in the manuscript.

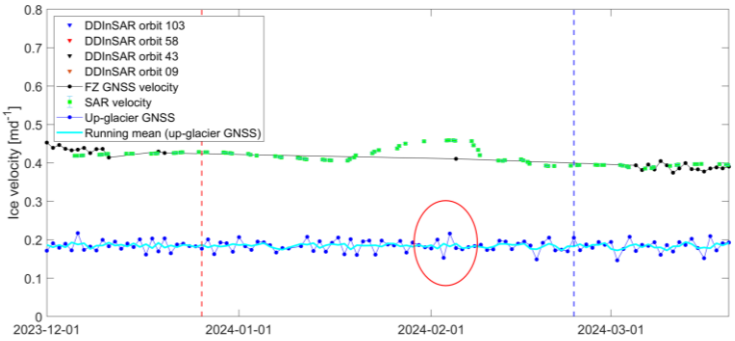

Fig. 9AR: SAR-derived velocity (green) and GNSS-derived velocity in the grounding zone (black), and ~15 km up glacier(blue) of the grounding zone.

Panel (c): Please change the pressure unit from "kPa" to hPa", which is the standard practical unit

We have changed the units on the plot.

Figure 3:
Panel (d): Please add a unit to the colorbar or in the caption. I think these are radians. It looks like there is a nice freely-floating area towards the end of the profiles, so please average the DInSAR displacement over some distance before the comparison to DSSH.

Yes, thank you, these are radians, which are dimensionless. We changed the label to "$-\pi$, π".
The reported DInSAR displacement values were averaged over the freely floating part of the transects.

Figure 4:
Move out of main text.

We retain panels d-f as we consider these results to be essential part of our analysis. Panels a-c were moved to the Appendix.

Figure 5:
Correcting the flexure curves for the "bending effect" would eliminate the spurious grounding-line migration within one local ice thickness (about plus/minus 300 m). Also, some flexure curves show distinct bumps upstream of the grounding line, which are indicative of viscoelasticity or grounding line migration between the SAR-data acquisitions. Why are the different shapes of the flexure curves not being discussed with respect to the timing (or tide, IBE) at the times of their underlying SAR scenes ?

We added the suggested discussion to the manuscript. We also added information about the mean vertical and horizontal errors due to bending to the figure caption, but we prefer to retain the DInSAR-derived displacement results here.

Figure 6:
Again, the main take-away is that including the IBE improves the correlation but the large RMSE are kept. Does this Figure need to be shown in the main text ?
Panel (a): cyan label: Reword to "Reconstructed SSH (tide-based only)" and black label to "Reconstructed SSH (tides plus IBE)"
Panels (b-e): Are unraveled (or single-tide) or DInSAR combination results plotted against each other ? I think it should be single tides, so the x-values would correspond to the red curve in panel a ? Is the x-label incorrect ?
Please swap the order of panel b/c and d/e, to match the description in L173 and logic of Fig.4

We removed panels related to the tide-based only analysis and change the primary focus of the figure to reconstruction analysis rather then the IBE. The updated figure is based on Fig. RA3 above.
The x-label is correct, these are differential displacements at SAR data acquisition times based on the reconstructed time series vs. DinSAR-derived displacements.
Panels d/e were removed.

Figure 7:
Is this separating parts of Fig. 4 d/e into steady/unsteady periods as defined by GNSS data as colors ? Another strength of the presented analysis, and I think the whole story about including the IBE to improve the statistics can easily be moved here by including two additional panels and moving Figs. 4 and 6 to the Appendix/SI.

Yes, it is. We prefer to move this figure, which generalizes results for all orbits, to the Appendix and keep Figure 8 in the main text to better demonstrate horizontal errors due to velocity variability and bending across the orbits.

Figure 8:
I don't think this figure adds to the storyline and can be summarized when presenting Fig. 7 in the main text. It should therefore also be moved to the Appendix/SI.

We prefer to retain this figure and remove Figure 7 instead, as explained in our response regarding Figure 7.

Figure 9:
For the reasons outlined above, temporarily integrating the data points by fitting a linear regression isn't physically motivated in the manuscript's current form. I think the panel (a) shows a signal that can be further explored, but since it doesn't add to the story Fig. 9 should therefore be removed from the manuscript.
We know from Schmeltz et al., 2002, and others that it's non-linear.

We removed this figure from the manuscript. Information about the flexure zone width and the distance to the hinge line is presented in table form instead.

Figure 10:
I was a bit confused if flexure zones or grounding zones are displayed in panel a and b-d ? I think it's grounding zone limits, please clarify.

"a)" is an example of flexure zone, b)-d) are grounding zones over observation period. We replaced a flexure zone in panel (a) with DInsAR-derived grounding zone to improve the figure clarity.

Figure 11:
Add "Hofmöller diagrams" at the start of the caption. Unify the labels to either m/d or m/yr. Also, add the location of the GNSS to one of the transects (consider a colored scatter with the same colormap, or its difference to the SAR-derived velocities through time). Interestingly, the acceleration in Jan/Feb 2024 occurs through the tidal-flexure zone. Was the signal investigated ?

We added "Hovmöller diagram of…" to the caption and the location of GNSS to the central transect.
The question about acceleration was answered above: this signal coincided with temperature rise and we think it is a real signal, but we have no other reliable confirmations.

References

Chien, Y., Zhou, C., Sun, S., Chen, Y., Wang, T., Zhang, B., 2026. Ephemeral grounding on the Pine Island Ice Shelf, West Antarctica, from 2014–2023. The Cryosphere 20, 245–263. https://doi.org/10.5194/tc-20-245-2026

Freer, B.I.D., Marsh, O.J., Hogg, A.E., Fricker, H.A., Padman, L., 2023. Modes of Antarctic tidal grounding line migration revealed by Ice, Cloud, and land Elevation Satellite-2 (ICESat-2) laser altimetry. The Cryosphere 17, 4079–4101. https://doi.org/10.5194/tc-17-4079-2023

Han, H., Lee, H., 2015. Tide-corrected flow velocity and mass balance of Campbell Glacier Tongue, East Antarctica, derived from interferometric SAR. Remote Sens. Environ. 160, 180–192. https://doi.org/10.1016/j.rse.2015.01.014

Li, T., Dawson, G.J., Chuter, S.J., Bamber, J.L., 2023. Grounding line retreat and tide-modulated ocean channels at Moscow University and Totten Glacier ice shelves, East Antarctica. The Cryosphere 17, 1003–1022. https://doi.org/10.5194/tc-17-1003-2023

Minchew, B.M., Simons, M., Riel, B., Milillo, P., 2017. Tidally induced variations in vertical and horizontal motion on Rutford Ice Stream, West Antarctica, inferred from remotely sensed observations. J. Geophys. Res. Earth Surf. 122, 167–190. https://doi.org/10.1002/2016JF003971

Padman, L., Erofeeva, S., Joughin, I., 2003. Tides of the Ross Sea and Ross Ice Shelf cavity. Antarct. Sci. 15, 31–40. https://doi.org/10.1017/S0954102003001032

Picton, H.J., Stokes, C.R., Jamieson, S.S.R., Floricioiu, D., Krieger, L., 2023. Extensive and anomalous grounding line retreat at Vanderford Glacier, Vincennes Bay, Wilkes Land, East Antarctica. The Cryosphere 17, 3593–3616. https://doi.org/10.5194/tc-17-3593-2023

Rack, W., King, M.A., Marsh, O.J., Wild, C.T., Floricioiu, D., 2017. Analysis of ice shelf flexure and its InSAR representation in the grounding zone of the southern McMurdo Ice Shelf. The Cryosphere 11, 2481–2490. https://doi.org/10.5194/tc-11-2481-2017

Ramanath, S., Krieger, L., Floricioiu, D., Diaconu, C.-A., Heidler, K., 2025. Automatic grounding line delineation of DInSAR interferograms using deep learning. The Cryosphere 19, 2431–2455. https://doi.org/10.5194/tc-19-2431-2025

Reeh, N., Christensen, E.L., Mayer, C., Olesen, O.B., 2003. Tidal bending of glaciers: a linear viscoelastic approach. Ann. Glaciol. 37, 83–89. https://doi.org/10.3189/172756403781815663

Rignot, E., Padman, L., MacAyeal, D.R., Schmeltz, M., 2000. Observation of ocean tides below the Filchner and Ronne Ice Shelves, Antarctica, using synthetic aperture radar interferometry: Comparison with tide model predictions. J. Geophys. Res. Oceans 105, 19615–19630. https://doi.org/10.1029/1999JC000011

Ross, N., Milillo, P., Nakshatrala, K.B., Ballarini, R., Stubblefield, A., Dini, L., 2024. Importance of ice elasticity in simulating tide-induced grounding line variations along prograde bed slopes. https://doi.org/10.5194/egusphere-2024-875

Schmeltz, M., Rignot, E., MacAyeal, D., 2002. Tidal flexure along ice-sheet margins: comparison of InSAR with an elastic-plate model. Ann. Glaciol. 34, 202–208. https://doi.org/10.3189/172756402781818049

Vaňková, I., Nicholls, K.W., Corr, H.F.J., Makinson, K., Brennan, P.V., 2020. Observations of Tidal Melt and Vertical Strain at the Filchner-Ronne Ice Shelf, Antarctica. J. Geophys. Res. Earth Surf. 125, e2019JF005280. https://doi.org/10.1029/2019JF005280

Wild, C.T., Alley, K.E., Muto, A., Truffer, M., Scambos, T.A., Pettit, E.C., 2022. Weakening of the pinning point buttressing Thwaites Glacier, West Antarctica. The Cryosphere 16, 397–417. https://doi.org/10.5194/tc-16-397-2022

Wild, C.T., Drews, R., Neckel, N., Lee, J., Kim, S., Han, H., Lee, W.S., Helm, V., Rosier, S.H.R., Marsh, O.J., Rack, W., 2025. Monitoring shear-zone weakening in East Antarctic outlet glaciers through differential InSAR measurements. The Cryosphere 19, 4533–4554. https://doi.org/10.5194/tc-19-4533-2025
Wild, C.T., Marsh, O.J., Rack, W., 2019. Differential interferometric synthetic aperture radar for tide modelling in Antarctic ice-shelf grounding zones. The Cryosphere 13, 3171–3191. https://doi.org/10.5194/tc-13-3171-2019
Wild, C.T., Marsh, O.J., Rack, W., 2018. Unraveling InSAR Observed Antarctic Ice-Shelf Flexure Using 2-D Elastic and Viscoelastic Modeling. Front. Earth Sci. 6, 28. https://doi.org/10.3389/feart.2018.00028
Wild, C.T., Marsh, O.J., Rack, W., 2017. Viscosity and elasticity: a model intercomparison of ice-shelf bending in an Antarctic grounding zone. J. Glaciol. 63, 573–580. https://doi.org/10.1017/jog.2017.15

References

Antropova, Y. K., Mueller, D., Samsonov, S. V., Komarov, A. S., Bonneau, J., & Crawford, A. J. (2024). Grounding-line retreat of Milne Glacier, Ellesmere Island, Canada over 1966–2023 from satellite, airborne, and ground radar data. Remote Sensing of Environment, 315, 114478. https://doi.org/10.1016/j.rse.2024.114478

Brunt, K. M., Fricker, H. A., Padman, L., Scambos, T. A., & O'Neel, S. (2010). Mapping the grounding zone of the Ross Ice Shelf, Antarctica, using ICESat laser altimetry. Annals of Glaciology, 51(55), 71–79. https://doi.org/10.3189/172756410791392790

Carnahan, E., Catania, G., & Bartholomaus, T. C. (2022). Observed mechanism for sustained glacier retreat and acceleration in response to ocean warming around Greenland. The Cryosphere, 16(10), 4305–4317. https://doi.org/10.5194/tc-16-4305-2022

Chartrand, A. M., Howat, I. M., Joughin, I. R., & Smith, B. E. (2024). Thwaites Glacier thins and retreats fastest where ice-shelf channels intersect its grounding zone. The Cryosphere, 18(11), 4971–4992. https://doi.org/10.5194/tc-18-4971-2024

Chen, H., Rignot, E., Scheuchl, B., & Ehrenfeucht, S. (2023). Grounding Zone of Amery Ice Shelf, Antarctica, From Differential Synthetic-Aperture Radar Interferometry. Geophysical Research Letters, 50(6), e2022GL102430. https://doi.org/10.1029/2022GL102430

Chien, Y., Zhou, C., Sun, S., Chen, Y., Wang, T., & Zhang, B. (2026). Ephemeral grounding on the Pine Island Ice Shelf, West Antarctica, from 2014–2023. The Cryosphere, 20(1), 245–263. https://doi.org/10.5194/tc-20-245-2026

Ciracì, E., Rignot, E., Scheuchl, B., Tolpekin, V., Wollersheim, M., An, L., Milillo, P., Bueso-Bello, J.-L., Rizzoli, P., & Dini, L. (2023). Melt rates in the kilometer-size grounding zone of Petermann Glacier, Greenland, before and during a retreat. Proceedings of the National Academy of Sciences, 120(20), e2220924120. https://doi.org/10.1073/pnas.2220924120

Costantini, M. (1998). A novel phase unwrapping method based on network programming. IEEE Transactions on Geoscience and Remote Sensing, 36(3), 813–821. https://doi.org/10.1109/36.673674

Forster, R. R., Rignot, E., Isacks, B. L., & Jezek, K. C. (1999). Interferometric radar observations of Glaciares Europa and Penguin, Hielo Patagónico Sur, Chile. Journal of Glaciology, 45(150), 325–337. https://doi.org/10.3189/S0022143000001829

Freer, B. I. D., Marsh, O. J., Hogg, A. E., Fricker, H. A., & Padman, L. (2023). Modes of Antarctic tidal grounding line migration revealed by Ice, Cloud, and land Elevation Satellite-2 (ICESat-2) laser altimetry. The Cryosphere, 17(9), 4079–4101. https://doi.org/10.5194/tc-17-4079-2023

Fricker, H. A., Coleman, R., Padman, L., Scambos, T. A., Bohlander, J., & Brunt, K. M. (2009). Mapping the grounding zone of the Amery Ice Shelf, East Antarctica using InSAR, MODIS and ICESat. Antarctic Science, 21(5), 515–532. https://doi.org/10.1017/S095410200999023X

Gadi, R., Rignot, E., Menemenlis, D., & Scheuchl, B. (2025). Contrasting melt regime in the Ice Grounding Zone of Thwaites Glacier, West Antarctica. Proceedings of the National Academy of Sciences, 122(48), e2512626122. https://doi.org/10.1073/pnas.2512626122

Holmes, F. A., Barnett, J., Åkesson, H., Morlighem, M., Nilsson, J., Kirchner, N., & Jakobsson, M. (2025). Sea level rise contribution from Ryder Glacier in northern Greenland varies by an order of magnitude by 2300 depending on future emissions. The Cryosphere, 19(7), 2695–2714. https://doi.org/10.5194/tc-19-2695-2025

Howard, S. and Padman, L. (2021). Gr1kmTM: Greenland 1 kilometer Tide Model, Arctic Data Center, https://doi.org/10.18739/A2251FM3S

Hu, J., Li, Z. W., Ding, X. L., Zhu, J. J., Zhang, L., & Sun, Q. (2014). Resolving three-dimensional surface displacements from InSAR measurements: A review. Earth-Science Reviews, 133, 1–17. https://doi.org/10.1016/j.earscirev.2014.02.005

Kim, J. H., Rignot, E., Holland, D., & Holland, D. (2024). Seawater Intrusion at the Grounding Line of Jakobshavn Isbræ, Greenland, From Terrestrial Radar Interferometry. Geophysical Research Letters, 51(6), e2023GL106181. https://doi.org/10.1029/2023GL106181

Le Meur, E., Sacchettini, M., Garambois, S., Berthier, E., Drouet, A. S., Durand, G., Young, D., Greenbaum, J. S., Holt, J. W., Blankenship, D. D., Rignot, E., Mouginot, J., Gim, Y., Kirchner, D., de Fleurian, B., Gagliardini, O., & Gillet-Chaulet, F. (2014). Two independent methods for mapping the grounding line of an outlet glacier – an example from the Astrolabe Glacier, Terre Adélie, Antarctica. The Cryosphere, 8(4), 1331–1346. https://doi.org/10.5194/tc-8-1331-2014

Li, T., Dawson, G. J., Chuter, S. J., & Bamber, J. L. (2023). Grounding line retreat and tide-modulated ocean channels at Moscow University and Totten Glacier ice shelves, East Antarctica. The Cryosphere, 17(2), 1003–1022. https://doi.org/10.5194/tc-17-1003-2023

Mannerfelt, E. S., Schellenberger, T., & Kääb, A. M. (2025). Tracking glacier surge evolution using interferometric SAR coherence—Examples from Svalbard. Journal of Glaciology, 71, e43. https://doi.org/10.1017/jog.2025.27

MDA Space (MDA). (2021). RADARSAT Constellation Mission (RCM) product specification. Retrieved from: https://download-telecharger.services.geo.ca/pub/csa_asc/Space-technology_Technologie-spatiale/radarsat_constellation_mission_plan/RCM-SP-52-9092_Product_Spec_1-15_Public.pdf

Millan, R., Mouginot, J., & Rignot, E. (2017). Mass budget of the glaciers and ice caps of the Queen Elizabeth Islands, Canada, from 1991 to 2015. Environmental Research Letters, 12(2), 024016. https://doi.org/10.1088/1748-9326/aa5b04

Milillo, P., Rignot, E., Mouginot, J., Scheuchl, B., Morlighem, M., Li, X., & Salzer, J. T. (2017). On the Short-term Grounding Zone Dynamics of Pine Island Glacier, West Antarctica, Observed With COSMO-SkyMed Interferometric Data. Geophysical Research Letters, 44(20), 10,436-10,444. https://doi.org/10.1002/2017GL074320

Milillo, P., Rignot, E., Rizzoli, P., Scheuchl, B., Mouginot, J., Bueso-Bello, J. L., Prats-Iraola, P., & Dini, L. (2022). Rapid glacier retreat rates observed in West Antarctica. Nature Geoscience, 15(1), Article 1. https://doi.org/10.1038/s41561-021-00877-z

Mohajerani, Y., Jeong, S., Scheuchl, B., Velicogna, I., Rignot, E., & Milillo, P. (2021). Automatic delineation of glacier grounding lines in differential interferometric synthetic-aperture radar data using deep learning. Scientific Reports, 11(1), Article 1. https://doi.org/10.1038/s41598-021-84309-3

Morlighem, M., Wood, M., Seroussi, H., Choi, Y., & Rignot, E. (2019). Modeling the response of northwest Greenland to enhanced ocean thermal forcing and subglacial discharge. The Cryosphere, 13(2), 723–734. https://doi.org/10.5194/tc-13-723-2019

Mortimer, C. A., Copland, L., & Mueller, D. R. (2012). Volume and area changes of the Milne Ice Shelf, Ellesmere Island, Nunavut, Canada, since 1950. Journal of Geophysical Research. Earth Surface; Washington, 117(4). http://dx.doi.org.proxy.library.carleton.ca/10.1029/2011JF002074

Padman, L., King, M., Goring, D., Corr, H., & Coleman, R. (2003). Ice-shelf elevation changes due to atmospheric pressure variations. Journal of Glaciology, 49(167), 521–526. https://doi.org/10.3189/172756503781830386

Pawlowicz, R., Beardsley, B., Lentz, S., 2002. Classical tidal harmonic analysis including error estimates in MATLAB using T_TIDE. Comput. Geosci. 28 (8), 929–937. https://doi.org/10.1016/S0098-3004(02)00013-4.

Picton, H. J., Stokes, C. R., Jamieson, S. S. R., Floricioiu, D., & Krieger, L. (2023). Extensive and anomalous grounding line retreat at Vanderford Glacier, Vincennes Bay, Wilkes Land, East Antarctica. The Cryosphere, 17(8), 3593–3616. https://doi.org/10.5194/tc-17-3593-2023

Porter, Claire, et al., 2023, "ArcticDEM, Version 4.1", https://doi.org/10.7910/DVN/3VDC4W, Harvard Dataverse, V1.

Rack, W., King, M. A., Marsh, O. J., Wild, C. T., & Floricioiu, D. (2017). Analysis of ice shelf flexure and its InSAR representation in the grounding zone of the southern McMurdo Ice Shelf. The Cryosphere, 11(6), 2481–2490. https://doi.org/10.5194/tc-11-2481-2017

Ramanath, S., Krieger, L., Floricioiu, D., Diaconu, C.-A., & Heidler, K. (2025). Automatic grounding line delineation of DInSAR interferograms using deep learning. The Cryosphere, 19(7), 2431–2455. https://doi.org/10.5194/tc-19-2431-2025

Rignot, E., Ciracì, E., Scheuchl, B., Tolpekin, V., Wollersheim, M., & Dow, C. (2024). Widespread seawater intrusions beneath the grounded ice of Thwaites Glacier, West Antarctica. Proceedings of the National Academy of Sciences, 121(22), e2404766121. https://doi.org/10.1073/pnas.2404766121

Rignot, E., Mouginot, J., & Scheuchl, B. (2011). Antarctic grounding line mapping from differential satellite radar interferometry. Geophysical Research Letters, 38(10). https://doi.org/10.1029/2011GL047109

Rignot, E., Padman, L., MacAyeal, D. R., & Schmeltz, M. (2000). Observation of ocean tides below the Filchner and Ronne Ice Shelves, Antarctica, using synthetic aperture radar interferometry: Comparison with tide model predictions. Journal of Geophysical Research: Oceans, 105(C8), 19615–19630. https://doi.org/10.1029/1999JC000011

Robel, A. A., Tsai, V. C., Minchew, B., & Simons, M. (2017). Tidal modulation of ice shelf buttressing stresses. Annals of Glaciology, 58(74), 12–20. https://doi.org/10.1017/aog.2017.22

Rocca, F., Prati, C., & Ferretti, A. (2010). Space-borne SARs: Impact of wavelengths and scan modes on ground motion studies. Annals of GIS, 16(2), 69–79. https://doi.org/10.1080/19475683.2010.492124

Ross, N., Milillo, P., Nakshatrala, K., Ballarini, R., Stubblefield, A., & Dini, L. (2025). Importance of ice elasticity in simulating tide-induced grounding line variations along prograde bed slopes. The Cryosphere, 19(6), 1995–2015. https://doi.org/10.5194/tc-19-1995-2025

Schoof, C. (2007). Ice sheet grounding line dynamics: Steady states, stability, and hysteresis. Journal of Geophysical Research: Earth Surface, 112(F3). https://doi.org/10.1029/2006JF000664

Sergienko, O. V. (2022). Marine outlet glacier dynamics, steady states and steady-state stability. Journal of Glaciology, 68(271), 946–960. https://doi.org/10.1017/jog.2022.13

Still, H., & Hulbe, C. (2021). Mechanics and dynamics of pinning points on the Shirase Coast, West Antarctica. The Cryosphere, 15(6), 2647–2665. https://doi.org/10.5194/tc-15-2647-2021

Tsai, V. C., & Gudmundsson, G. H. (2015). An improved model for tidally modulated grounding-line migration. Journal of Glaciology, 61(226), 216–222. https://doi.org/10.3189/2015JoG14J152

Van Wychen, W. V., Burgess, D., Kochtitzky, W., Nikolic, N., Copland, L., & Gray, L. (2020). RADARSAT-2 Derived Glacier Velocities and Dynamic Discharge Estimates for the Canadian High Arctic: 2015–2020. Canadian Journal of Remote Sensing, 46(6), 695–714. https://doi.org/10.1080/07038992.2020.1859359

Wallis, B. J., Hogg, A. E., Zhu, Y., & Hooper, A. (2024). Change in grounding line location on the Antarctic Peninsula measured using a tidal motion offset correlation method. The Cryosphere, 18(10), 4723–4742. https://doi.org/10.5194/tc-18-4723-2024

Wild, C. T., Drews, R., Neckel, N., Lee, J., Kim, S., Han, H., Lee, W. S., Helm, V., Rosier, S. H. R., Marsh, O. J., & Rack, W. (2025). Monitoring shear-zone weakening in East Antarctic outlet glaciers through differential InSAR measurements. The Cryosphere, 19(10), 4533–4554. https://doi.org/10.5194/tc-19-4533-2025

Wild, C. T., Marsh, O. J., & Rack, W. (2019). Differential interferometric synthetic aperture radar for tide modelling in Antarctic ice-shelf grounding zones. The Cryosphere, 13(12), 3171–3191. https://doi.org/10.5194/tc-13-3171-2019

Wild, C. T., Marsh, O. J., & Rack, W. (2018). Unraveling InSAR Observed Antarctic Ice-Shelf Flexure Using 2-D Elastic and Viscoelastic Modeling. Frontiers in Earth Science, 6. https://doi.org/10.3389/feart.2018.00028

Wood, M., Rignot, E., Fenty, I., An, L., Bjørk, A., van den Broeke, M., Cai, C., Kane, E., Menemenlis, D., Millan, R., Morlighem, M., Mouginot, J., Noël, B., Scheuchl, B., Velicogna, I., Willis, J. K., & Zhang, H. (2021). Ocean forcing drives glacier retreat in Greenland. Science Advances, 7(1), eaba7282. https://doi.org/10.1126/sciadv.aba7282

Wunsch, C., & Stammer, D. (1997). Atmospheric loading and the oceanic “inverted barometer” effect. Reviews of Geophysics, 35(1), 79–107. https://doi.org/10.1029/96RG03037